Cement and Concrete Research 176 (2024) 107411

Contents lists available at ScienceDirect

Cement and Concrete Research

journal homepage: www.elsevier.com/locate/cemconres

Performance improvement of Portland-limestone cement by mechanochemical activation

Jihoon Lee [a], Barbara Lothenbach [b,c], Juhyuk Moon [a,d,*]

[a] Department of Civil and Environmental Engineering, Seoul National University, Seoul 08826, Republic of Korea
[b] Empa, Laboratory for Concrete & Asphalt, Überlandstrasse 129, CH-8600 Dübendorf, Switzerland
[c] NTNU, Department of Structural Engineering, Trondheim, Norway
[d] Institute of Construction and Environmental Engineering, Seoul 08826, Republic of Korea

ARTICLE INFO

Keywords:
Portland limestone cement
Alkanolamine
Monocarboaluminate
Ferrite
Specific surface area

ABSTRACT

This study investigates mechanochemical activation with alkanolamine-based agents for improving the material performance of Portland-Limestone Cement (PLC). By using 0.1 wt% of diethanolisopropanolamine during grinding process, a noticeable improvement of compressive strength (>100 % increase in 28 days) was confirmed for PLC containing 20 % limestone due to the favorable interaction between the diethanolisopropanolamine and limestone. Grinding in the presence of diethanolisopropanolamine (1) enlarges the specific surface area when limestone is added, (2) stabilizes ettringite, (3) enhances hydration of ferrite, and (4) leads to form denser hydration products. The hydration of mechanochemically treated cement lowers the formation of portlandite with preferred orientation in (001) direction and leads to more formation of amorphous and AFm phases, independent of the presence of limestone. The limestone powder in mechanochemically activated PLC enhances the ferrite dissolution and the production of monocarbonate, which contributes to the significant improvement of compressive strength.

1. Introduction

Given the potential supply problem of conventional supplementary cementitious materials (SCMs) such as fly ash or ground granulated blast-furnace slag (GGBFS), the involvement of limestone in Portland cement has been a point of discussion [1,2]. Indeed, from the perspective of its sufficient supply, Portland-Limestone Cement (PLC) can contribute to lowering CO_2 emissions by reducing clinker production. In practice, many specifications allow Portland cement to contain 5 % limestone since the small amount of limestone substitution barely has any negative effect on its mechanical properties and durability compared to the cement without limestone [3]. For instance,

At low replacement, the limestone powder not only can enhance the hydration of clinker by the so-called filler effect but also reacts with C_3A in cement, producing hemicarbonate (Hc) and monocarbonate (Mc), contributing to compressive strength [4]. Since the permissible limestone contents, which do not decrease compressive strength, depend on the amount of alumina in binder materials, Using SCMs that include high alumina contents (e.g., GGBFS, metakaolin) can increase its contents with no compressive strength drop (even up to 10 % replacement) [5]. Nevertheless, it is required to involve limestone powder in PLC at levels exceeding 10 % to reduce CO_2 emissions. For instance, EN 197–1 designates two classes of PLC as CEM II/A-L and CEM II/B-L, with a maximum limestone content of 20 % and 35 %, respectively. However, these amounts of limestone substitution, unfortunately, induce defective mechanical properties and durability in concretes [5,6].

Meanwhile, Assorted types of alkanolamine have recently been studied, particularly their use as additives and grinding agent (GA) for an efficient milling process. It was reported that triethanolamine (TEA) can increase the early strength at low dosages (0.01–0.1 %), especially during the first day of hydration, by accelerating the dissolution of C_3A and C_4AF and the formation of ettringite. Conversely, the later age strength is diminished as the adsorption of TEA on C_3S surface prevents further hydration [7–11]. Although triisopropanolamine (TIPA) decreases the early compressive strength due to the introduction of gas into the cement matrix by lipophilicity of methyl groups, it can increase the later compressive strength by enhancing the dissolution of C_4AF through the complexation with Fe^{3+} ions [12,13]. In addition, Gartner and Myers demonstrated that the compressive strength increased with C_4AF contents when TIPA was used [11]. TIPA has a higher steric hindrance

* Corresponding author at: Department of Civil and Environmental Engineering, Seoul National University, Seoul 08826, Republic of Korea.
E-mail address: juhyukmoon@snu.ac.kr (J. Moon).

https://doi.org/10.1016/j.cemconres.2023.107411
Received 27 May 2023; Received in revised form 29 November 2023; Accepted 17 December 2023
Available online 23 December 2023

Table 1
Chemical composition of the materials.

Chemical composition [g/100 g]	CC (g)	Limestone powder (g)	Gypsum (g)
CaO	64.80	45.32	34.9
SiO_2	21.90	11.30	1.52
Al_2O_3	5.33	1.59	0.62
Fe_2O_3	3.02	0.52	0.24
MgO	2.83	1.99	0.57
K_2O	0.83	0.56	0.06
SO_3	0.53	0.62	43.78
TiO_2	0.28	0.07	< 0.01
P_2O_5	0.21	0.06	< 0.01
Loss of ignition	< 0.01	37.80	18.20

Table 2
Phase composition of materials.

Phase composition [g/100 g]	CCPC (%)	Limestone powder (%)
Alite	51.4	–
Belite	28.6	–
Aluminate	4.0	–
Ferrite[a]	11.2	–
Periclase	2.5	–
Lime	1.3	–
Arcanite	0.6	–
Calcite	–	86.3
Quartz	0.2	10.0
Dolomite	–	2.9
Zeolite[b]	–	0.4

[a] Al:Fe = 1.1:0.9.
[b] Zeolite structure type RUB-3 [31].

Table 3
Mixture proportions.

Mixture	CC (g)	Gypsum (g)	Limestone powder (g)	DEIPA (wt%)
LS0_0	95	5	–	–
LS0_0.1	95	5	–	0.1
LS10_0	85	5	10	–
LS10_0.1	85	5	10	0.1
LS20_0	75	5	20	–
LS20_0.1	75	5	20	0.1

compared to TEA, leading to elevated concentration of TIPA in the pore solution until a later age and lasting hydration of C_3S and C_4AF [14].

Furthermore, a new type of alkanolamine has recently been investigated for improving the aluminate reaction; diethanolisopropanolamine (DEIPA). Ma et al. found that the hydration of C_4AF considered less reactive materials among clinker phases increased with the dosage of DEIPA (0.02–0.1 %) [15]. Further, with the addition of 0.05 % DEIPA, the compressive strength of mortar slightly increased, while it decreased with 0.5 % DEIPA after 28 days [16]. Lu et al. reported that DEIPA, especially, has a strong complexation capability with Fe^{3+} ions, resulting in the acceleration of C_4AF dissolution after sulfate depletion. It was also observed that DEIPA retard silicate reaction at a high dosage (0.5 %), but not at 0.1 % dosage [17].

Although there are some studies on various GA as listed above, these agents were generally dissolved in mixing water prior to experiments in those studies. However, in the actual cement manufacture process, GA is applied in the final "grinding process" [18–20]. As GAs have both chemical as well as physical impacts (i.e., mechanochemical) on the cement hydration, experiments based on the admixture-type test could underestimate the mechanochemical impacts of the GAs. Only a few studies have shown the effect of mechanochemical activation by using alkanolamines during the grinding process [21–23]. Moreover, although the presence of limestone powder could increase the fineness of the binder [24], there are no reported trials or studies for enhancing the performance of PLC through mechanochemical activation using GA.

In particular, the aim of this paper is to analyze the mechanochemical impacts on limestone blended cement with the different substitutions of limestone under the use of DEIPA as GA. Given that the enhancement of C_4AF reactivity by DEIPA is pronounced compared to other alkanolamines and this can lead to the formation of AFm phases (Eqs. (1)–(3)), DEIPA was used as GA in this study [17].

Reaction with gypsum

$$C_4AF + 3C\bar{S}H_2 + 30H \rightarrow C_6A\bar{S}_3H_{32} + FH_3 + CH \quad (1)$$

$$C_4AF + C_6A\bar{S}_3H_{32} + 12H \rightarrow 3C_4A\bar{S}H_{12} + 2FH_3 + 2CH \quad (2)$$

Reaction with calcite

$$C_4AF + Cc + 14H \rightarrow C_4AcH_{11} + FH_3 \quad (3)$$

Assorted experiments were carried out to elucidate the origins of strength improvement, including isothermal conduction calorimetry, X-ray diffraction (XRD) with quantitative Rietveld refinement, and thermogravimetric (TG) analysis. The Blaine air permeability method and particle laser analyzer were also used to confirm the physical changes after grinding with DEIPA. Lastly, thermodynamic modeling was employed to further understand the hydration process as a result of the well-designed experiments.

2. Materials and experimental methods

2.1. Materials

Firstly, since the main experimental variable in this paper is the amount of limestone substitution, it is necessary to intentionally produce a limestone-free control sample. Therefore, Pre-crushing clinker (without gypsum or other additives) was calcined at 850 °C for 3 h to remove any calcite and filtered out through a No. 30 (600μm) sieve. Then, gypsum, limestone powder, and DEIPA were blended with the calcined pre-crushing clinker (CC). The composites were ground using a McCrone micronizing mill (McCrone Scientific Ltd., London, UK) for 15 min. The size reduction of the binder was simply carried out by friction and impact between the grinding mills and the powder during the grinding process. A particle size analyzer (Malvern Instrument. Ltd., UK) was employed to assess the effect of DEIPA on the particle size distribution and the results of the Blaine specific surface area (SSA) were compared with particle size distribution.

The chemical and mineralogical compositions of the materials were represented in Table 1 and Table 2 obtained from X-ray fluorescence (XRF) and XRD/Rietveld analysis [25]. Given that the C_4AF content in XRD measurement (i.e., 11.2 %) was quite high compared to that in XRF (i.e., 9.19 % by Bogue calculation), it was estimated that the Al to Fe ratio in C_4AF should be corrected. In order to remove the silicate phases (C_3S and C_2S) from CC, a selective dissolution method was carried out using the maleic acid [26]. Then, the XRD pattern of the powder without silicate phases was obtained and the occupancy parameters of Al and Fe atoms in C_4AF were refined [27,28]. Further, the unit cell and full width at half maximum (FWHM) parameters were refined within 1 % of the variation ratio [29,30], resulting in that the Al-to-Fe ratio of C_4AF was 1.1:0.9.

2.2. Methods

2.2.1. Sample preparation

Deionized water was used to prepare pastes with a water to binder ratio (W/B) of 0.5. They were then cured in a constant temperature/humidity environment at 20 °C with 60 % humidity for 6 and 12 h, and 1, 3, 7 and 28 days. The details of mixture proportions are shown in Table 3. mixture proportions The dosage of DEIPA was fixed to the 0.1 % of the binder because the reactivity of C_4AF was improved as DEIPA dosage increased up to 0.1 % and this dosage did not induce the

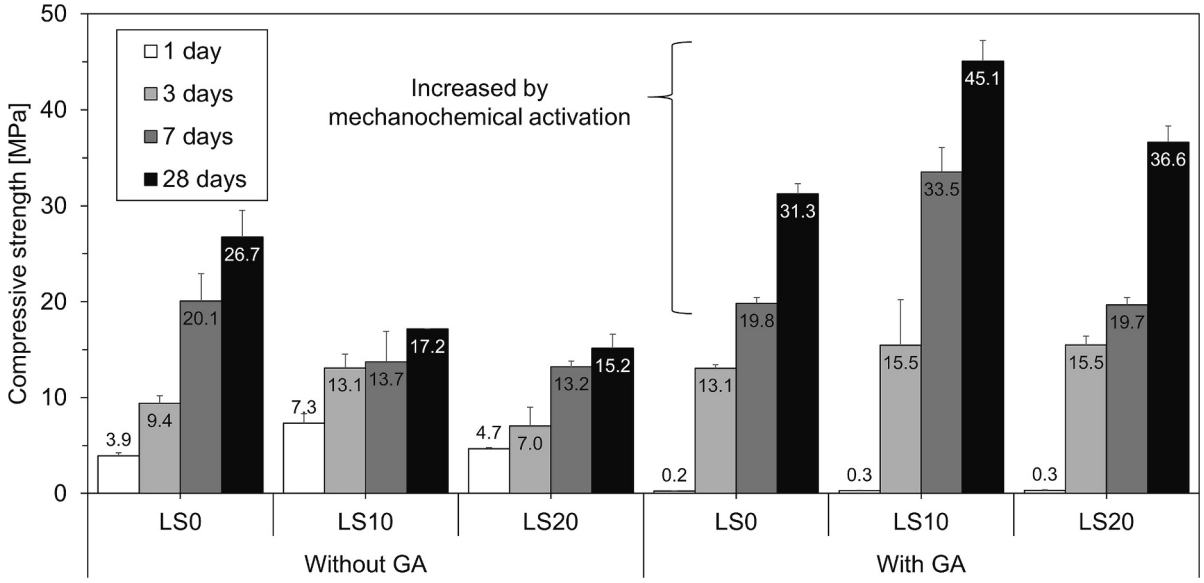

Fig. 1. Compressive strength of pastes with W/B = 0.5, without and with limestone (LS0, LS10 and LS20) and without or with 0.1 % DEIPA.

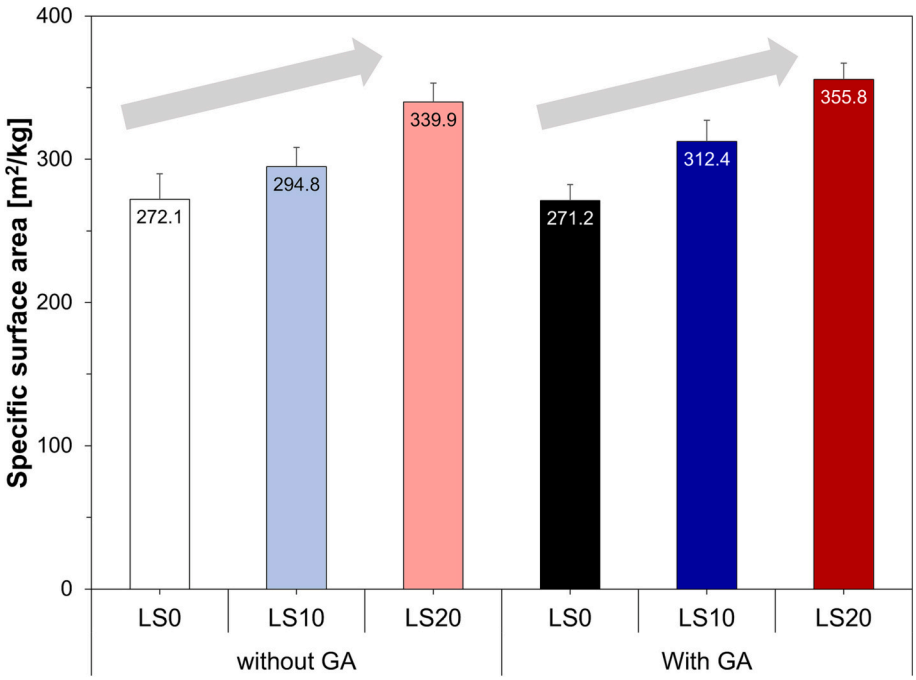

Fig. 2. Results of the Blaine surface area test.

significant retardation on silicate reaction [15,17]. Isothermal conduction calorimetry, XRD, DSC-TG and compressive strength tests were conducted with these cement pastes. In particular, the compressive strength tests were carried out with the pastes, which were molded in cubic shape, then, demolded after 1 day of hydration. For XRD and DSC-TG tests, the hydrated powders were immersed in isopropyl alcohol and ethyl ether to stop the hydration reaction by removing free water from the cement paste. The ethyl ether was then evaporated by drying up to 40 °C for 40 min [32–34].

2.2.2. Isothermal calorimetry

The heat of hydration of the pastes with or without GA was measured using a TAM Air system (TA Instruments, USA) at 20 ±0.02 °C. A steady baseline was maintained for 2 h at a constant external room temperature, 20 °C, before the measurement. Deionized water was added to each mixture already ground with or without GA. Subsequently, the cement paste was mixed externally for 2 min before pouring it into glass ampoules. The glass ampoules were then sealed with aluminum lids and placed into a calorimeter. The heat released from pastes was assessed for 3 days to observe the effect of mechanochemical activation on PLC hydrations.

2.2.3. Thermogravimetry analysis

TG analysis was carried out to identify and quantify not only the hydration products but also chemically bound water, which was used for normalizing the XRD/Rietveld results to anhydrous cement [35,36]. The change in paste weight based on the increase in temperature was gauged by SDT Q600 (TA Instrument, Ltd., USA) heating from 20 °C to 1000 °C.

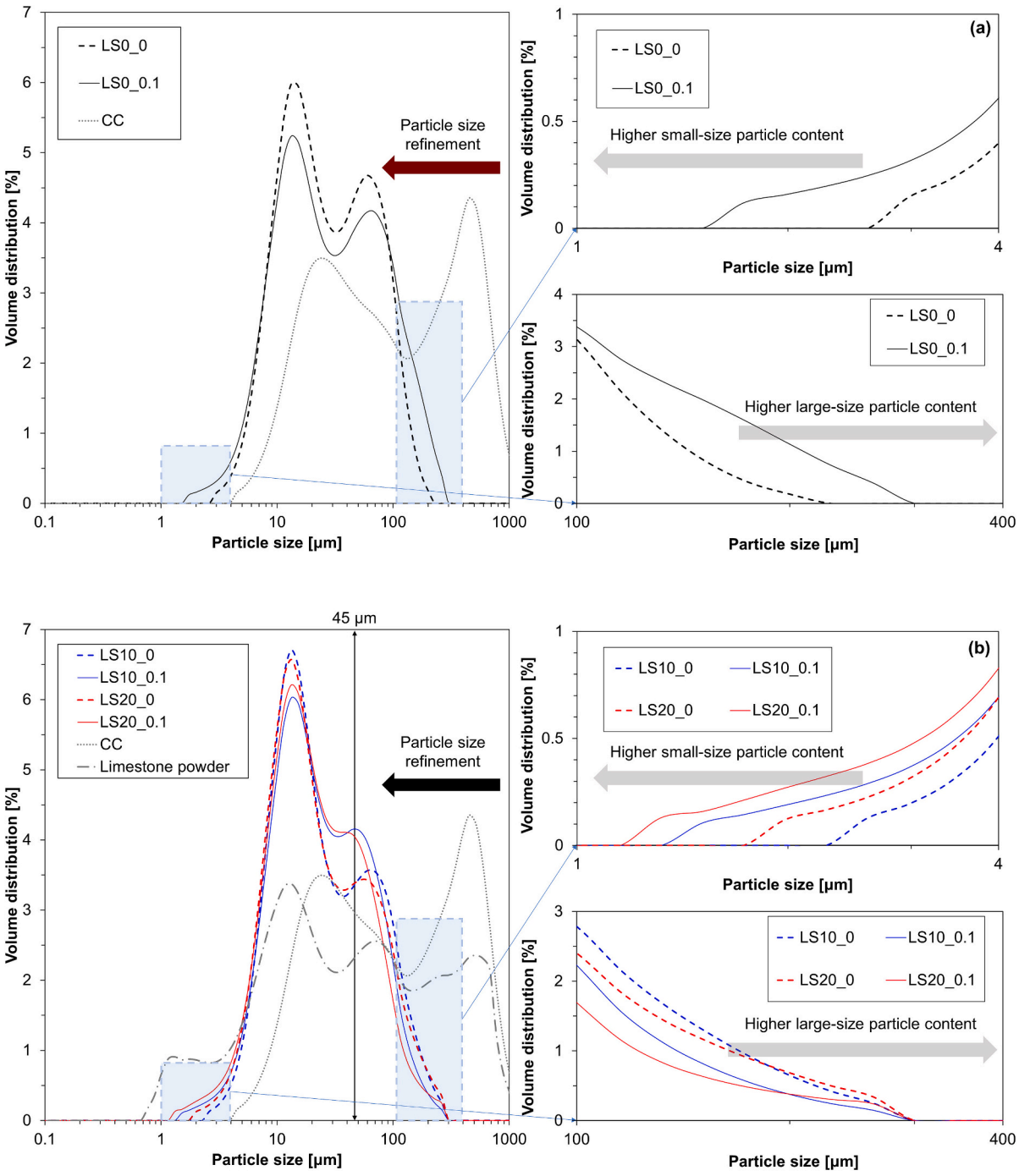

Fig. 3. Particle size distribution of raw materials and ground binder with and without a grinding agent (a) without limestone powder, (b) with limestone powder.

The heating rate was 10 °C/min with a N_2 gas flow rate of 100 mL/min. The amount of CH was obtained using below equation. $w_{weight\ loss}$ was determined by using tangential method [35]. Then, the content of CH was normalized by g of anhydrous binder, using the dry weight at 550 °C (w_{550}).

$$\mathrm{CH\ (wt\%)} = \frac{w_{weight\ loss}}{w_{550}} \times \frac{74}{18} \tag{4}$$

2.2.4. X-ray diffraction/Rietveld method

The XRD data were measured using a D2 phaser X-ray diffractometer (Bruker Co. Ltd., Germany) equipped with Cu-Kα radiation (λ = 1.5418 Å) in the range of 2θ between 5° and 60°. The collected XRD data were analyzed using X'pert HighScore Plus software 4.8 (PANalytical, Netherlands) with the inorganic crystal structure database (ICSD) [37] and the crystallography open database (COD) [38]. The amorphous phase was calculated using TiO_2 (SRM 674b, NIST, US) as the internal standard material at a weight ratio of paste: TiO_2 = 9:1 [39]. Each amount of hydration products and anhydrous clinkers was expressed as % of w_{550} (Eqs. (5)) [36].

$$\mathrm{M_{dry}} = \frac{M_{measured}}{1 - H_2O_{bound}} = \frac{M_{measured}}{w_{550}} \tag{5}$$

2.2.5. Selective dissolution

The major phases of hydration products can be dissolved in the cement matrix by selective dissolution to identify minor phases in

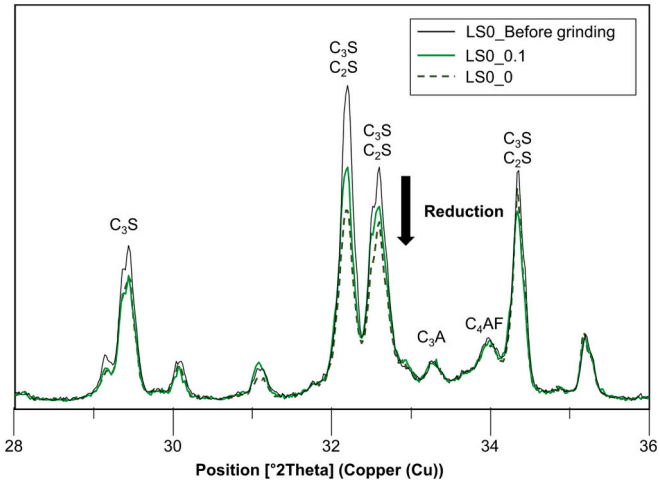

Fig. 4. X-ray diffraction patterns of the cement without limestone before and after grinding with or without grinding agent.

hydrated cement. A salicylic acid/methanol (SAM) extraction allows for the dissolution of C_3S, C_2S, CH, C-S-H, AFt, and AFm phases, leaving C_4AF, Fe-siliceous hydrogarnet, and hydrotalcite in the cement matrix [40,41]. 30 g of salicylic acid dissolved in 300 ml of methanol and, 5 g of hydrated cement was added. The mixture was, then, stirred for 5 h, and the suspension was then settled for 15 min before filtering it. The slurry was washed with methanol and heated at 90 °C for 45 min.

2.2.6. Thermodynamic modeling

The phase assemblage of the PLC system was calculated based on the experimentally obtained degree of hydration on 28 days hydration, using the Gibbs free energy minimization software, GEM-Selektor v.3.9.5 [42,43]. In addition to the built-in standard thermodynamic database [44], thermodynamic data for cement hydrates from the Cemdata 18 were added. C-S-H model used in this paper was CSHQ model because the uptake of minor cations such as Na-, K-, and Sr- in C-S-H was not expected and alkali activation was not applied in this experiments [45,46].

The extended Debye-Hückel equation [47] was applied to calculate the activity coefficients for aqueous species in the cement system, given as Eqs. (6).

$$log_{10}\gamma_i = \frac{-A_\gamma z_i^2\sqrt{I}}{1+\dot{a}B_\gamma\sqrt{I}} + b_\gamma I + log_{10}\frac{X_{jw}}{X_w} \quad (6)$$

where γ_i and z_i refer to the activity coefficient and charge of the i^{th} aqueous species, respectively; A_γ is a temperature coefficient; B_γ is a pressure coefficient; I means the molar ionic strength of the pore solution; X_{jw} is the molar quantity of water; X_w is the total molar amount of the aqueous phase; $\dot{a}$ and b_γ are a common ion size parameter, and a short-range interaction parameter, each. $\dot{a}$ was set to 3.67 Å and b_γ was

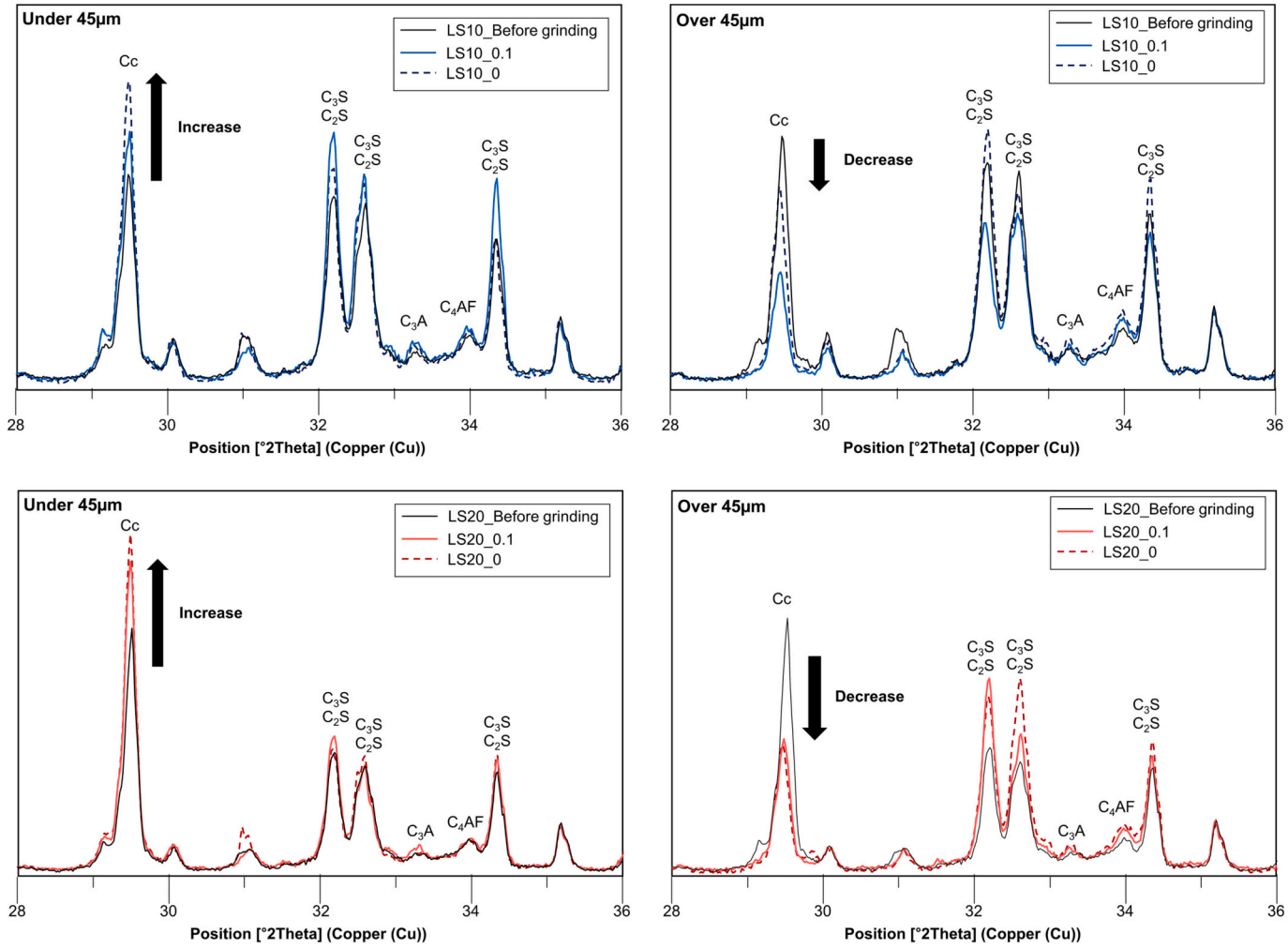

Fig. 5. X-ray diffraction patterns of limestone-containing cement before and after grinding with or without grinding agent. The ground samples were divided into two according to particle size.

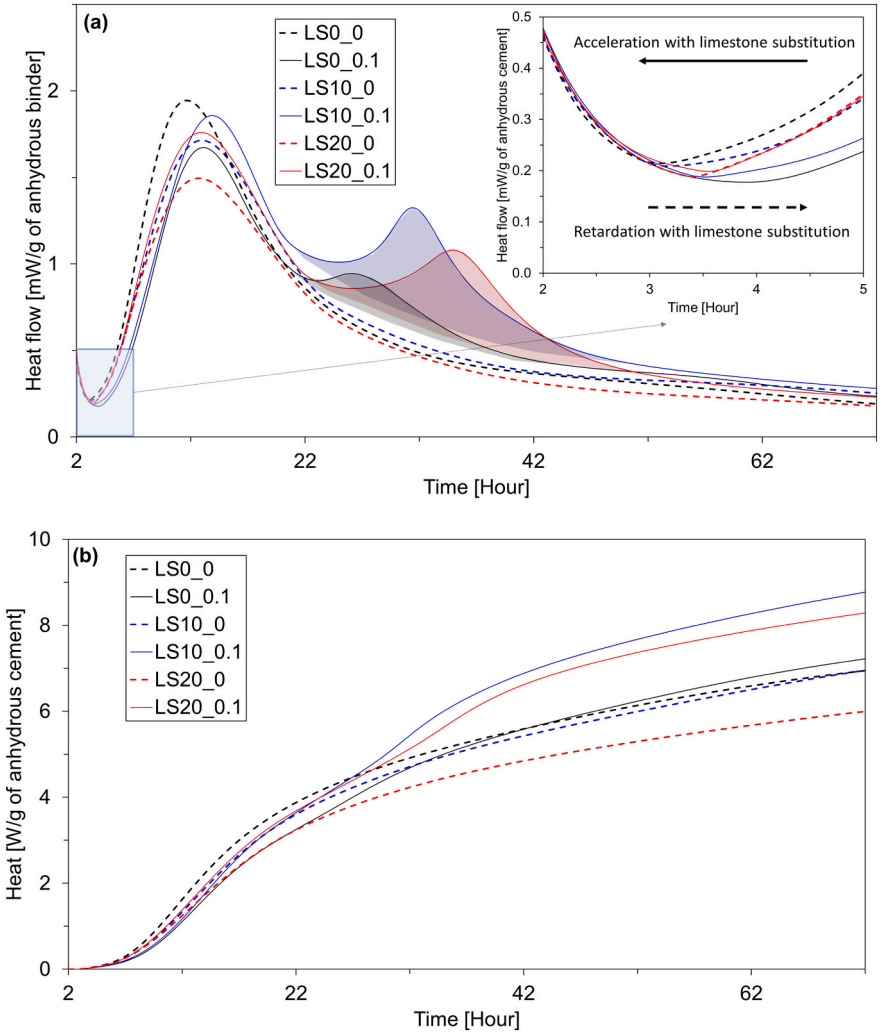

Fig. 6. Heat flow development (a) of samples versus times between 0 h and 72 h and (b) cumulative heat. All data was normalized by g of binder (i.e., CC+ gypsum + limestone powder).

determined to 0.123 kg/mol to simulate KOH dominated electrolyte aqueous solution [4,48]. In this simulation, the temperature and pressure were set to 20 °C and 1 bar, respectively.

3. Results

3.1. Compressive strength development

Fig. 1 depicts the compressive strength of the cement pastes. In the absence of DEIPA, the strength of PLC was similar to or over that of LS0 until 3 days of hydration but not after 7 days of hydration. Severe strength drop with limestone substitution was observed at the later age.

On the other hand, in the presence of DEIPA, no strength was gained on the first day regardless of the presence of limestone powder. However, the compressive strength of pastes with DEIPA exceeded those without DEIPA at the same limestone substitution from 3 days and onwards. Even, a remarkable improvement in compressive strength was observed at later ages, especially for PLC. Despite 20 % limestone substitution, the compressive strength of PLC was equal to or even higher than that of 0 % limestone.

The compressive strength of PLC was directly influenced by the alumina content Therefore, Ramezanianpour and Hooton reported that the cement mortar blended with SCMs containing high alumina content could achieve maximum compressive strength with the involvement of limestone powder. However, the optimum limestone content to increase or maintain compressive strength was up to 10 % [6]. Thus, in this study, the mechanochemical activation by DEIPA increased the available alumina content, leading to no deficit in the compressive strength even up to 20 % limestone substitution.

3.2. Mechanical effect of grinding agent

3.2.1. Blain specific surface area and particle size distribution

Fig. 2 displays the Blaine SSA of the binder after grinding process. In the absence of limestone powder, the effect of DEIPA on grinding seemed to be insignificant as no difference between SSA of LS0_0 and LS0_0.1 was observed. However, at the same amount limestone powder, the use of DEIPA increased the SSA. Moreover, it increased with the limestone substitution because of the higher grindability of limestone powder [24]. Thus, LS20_0.1 had the highest SSA among all ground binders.

Fig. 3 (a) and (b) present the particle size distribution of raw materials and the mixtures after grinding with DEIPA and without DEIPA. The particle size refinement after grinding was observed in all mixtures. In the absence of limestone powder, using DEIPA as GA increased the portion of particles with smaller than 10 μm and bigger than 100 μm while the fraction of particles between 10 μm and 100 μm decreased. These results corresponded with the result of Li et al., in which they described the increase of large particles as by the aggregation of fine clinker particles because DEIPA stuck to the surface of clinker and

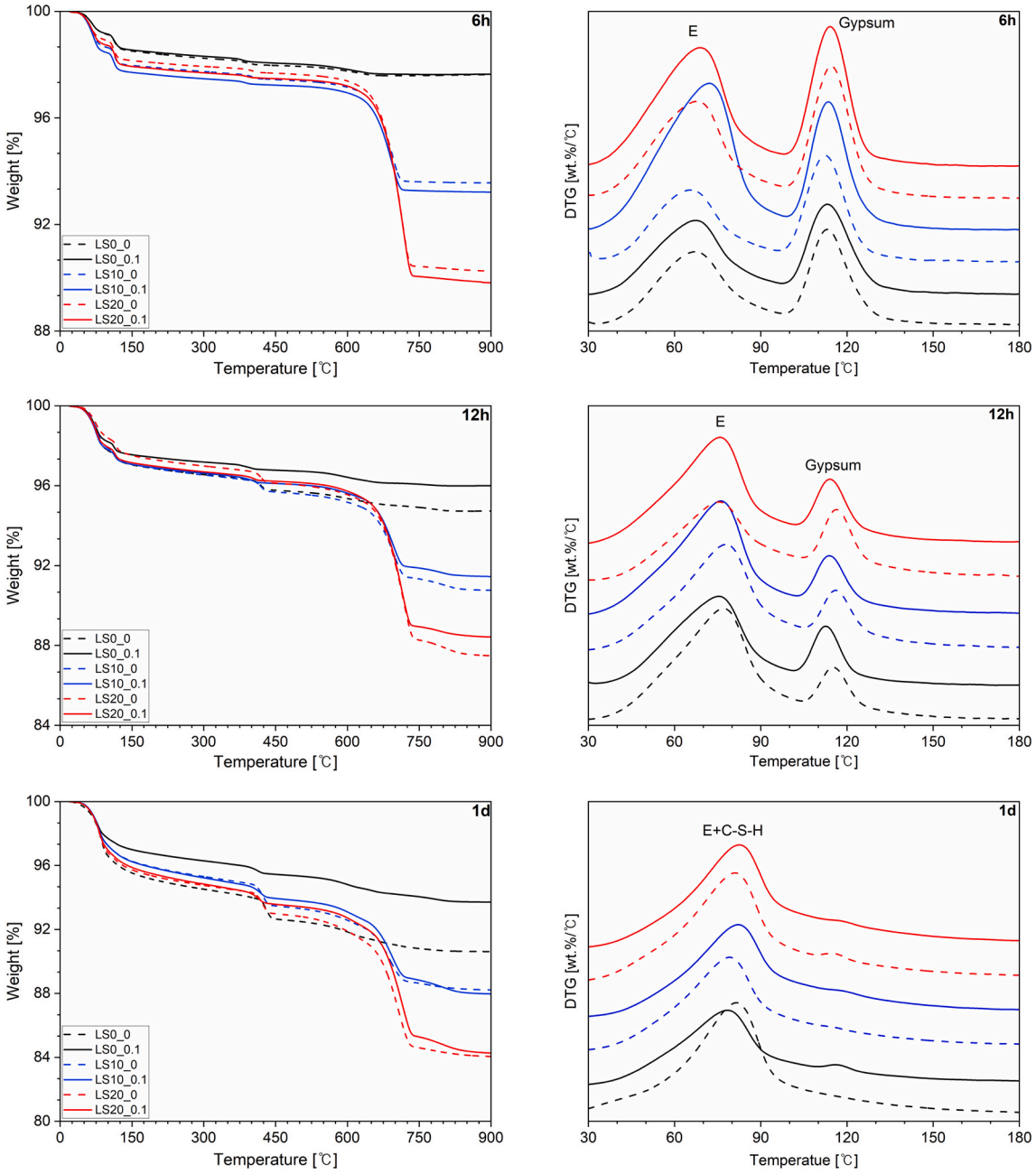

Fig. 7. TG and DTG data of hydrated cement without and with limestone (LS0, LS10 and LS20) and without or with 0.1 % DEIPA after 6 and 12 h, 1, 3, 7, and 28 days.

generated electrostatic charges [21].

Meanwhile, in the presence of limestone powder, mechanochemical activation on PLC had a different effect with that without limestone. As shown in Fig. 3 (b), using DEIPA decreased the fraction of large particles (i.e., bigger than 100 μm) but increased the portion of small particles (i.e., smaller than 10 μm), leading to the SSA enlargement (Fig. 2), indicating that the use of DEIPA is quite effective for grinding PLC.

3.2.2. *X-ray powder diffraction*

The change in XRD patterns of the cement without limestone before and after grinding is shown in Fig. 4. It should be noted that calcium sulfate type (e.g., hemihydrate or anhydrite) after grinding can affect the cement hydration [49]. However, the decomposition of gypsum was not observed possibly due to the short grinding time. The intensities of clinker phases, especially silicate phases, were reduced after grinding regardless of the use of GA. Thus, in the absence of limestone powder, the reduction of peak intensity was more significant in LS0_0 than in LS0_0.1.

The change in XRD pattern of PLC before and after grinding is presented in Fig. 5. The particles with 45 μm diameter increased in PLC after grinding with DEIPA, which was quite opposite to the binder without limestone. Therefore, the ground PLC were divided into two by passing through the No. 325 sieve (45 μm), and then, XRD was conducted for each mixture (i.e., bigger than 45 μm and smaller than 45 μm), respectively.

In the 10 % limestone powder substitution regardless of the DEIPA, more calcite was detected in the mixture <45 μm diameter. In the presence of DEIPA, more amount of C_3S was observed in the particles

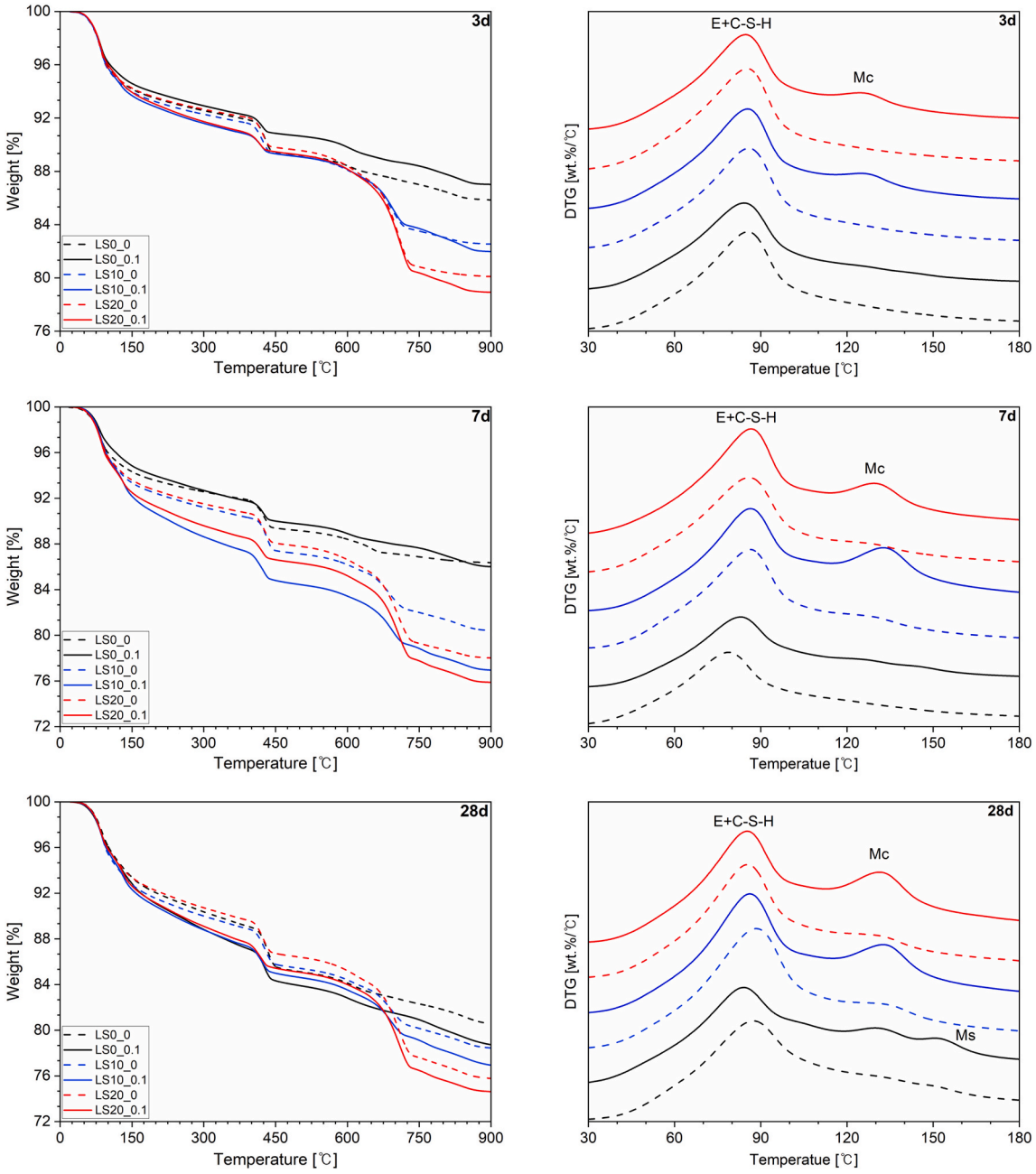

Fig. 7. (*continued*).

with size under 45 μm while C_3S decreased in the large particles. Therefore, it can be concluded that the grindability of limestone is more pronounced than that of clinker which helps pulverizing C_3S under the use of DEIPA.

In the 20 % limestone powder substitution, similar to the 10 % limestone replacement, more calcite was identified in the smaller particles after grinding regardless of the DEIPA application. Conversely, clinker remained in the larger particle in both grinding processes. It might be because the grinding time was too short to pulverize clinker in terms of the larger limestone powder contents (i.e., 20 %), and limestone powder was crushed firstly in PLC.

3.3. Chemical effect of grinding agent

3.3.1. Hydration kinetics

Fig. 6 (a) and (b) presents the heat flow and cumulative heat during 3 days of hydration. The heat flow showed the onset of the main hydration peak after approximately 3 h. In the absence of DEIPA, the onset of hydration was retarded with the limestone replacement, which was because the ratio of gypsum to clinker increased as more limestone powder was replaced (Table 3). In addition, no clear shoulder or peak of secondary hydration was observed. The heat generated per g of binder decreased as expected due to the substitution of more limestone (i.e., dilution effect) after 2 days of hydration.

Vance et al. reported that a 10 % replacement of the limestone powder with a medium diameter of 15 μm had no significant impact on the hydration kinetic [50]. Moreover, Briki et al. carried out heat flow experiments with 20 % limestone substitution, in which the dilution effect of clinker led to the low heat emission, especially, when the coarse limestone powder was replaced [51], which is in agreement with the results of this paper.

On the other hand, in the presence of DEIPA use, although the onset

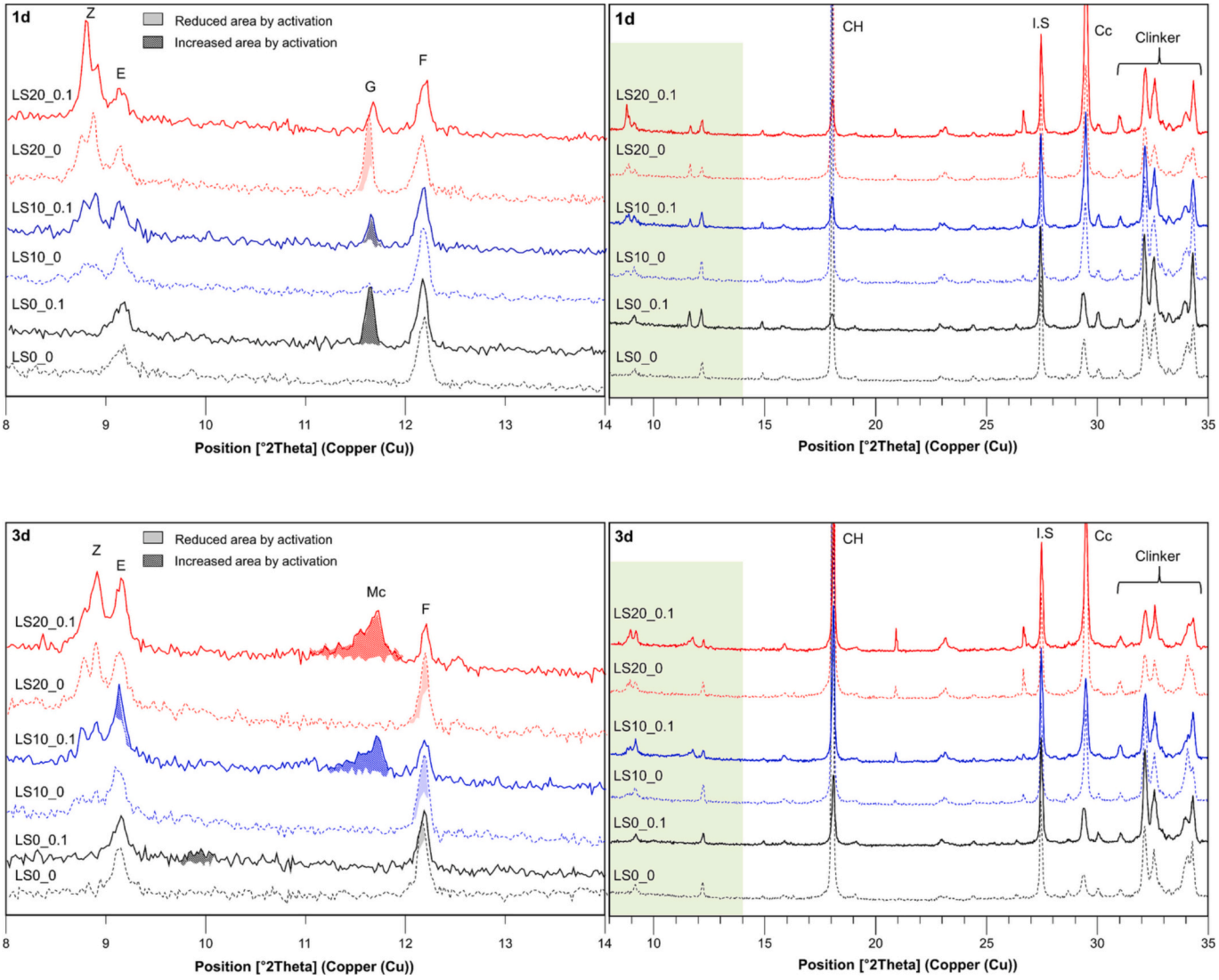

Fig. 8. XRD patterns of hydrated PLC paste samples after 1, 3, 7 and 28 days (CH: portlandite, I·S: internal standard materials (TiO_2), Cc: calcite, Z: zeolite, present in the limestone used, E: ettrinigte, F: ferrite, G: gypsum, Hc: hemicarbonate, Mc: monocarbonate, Ms.: monosulfate).

of hydration was retarded at the same limestone substitution, the hydration was accelerated as the limestone powder substitution increased. Furthermore, a secondary hydration peak after sulfate depletion was clearly visible, indicating that mechanochemical activation enhanced the aluminate reaction. The second peak of LS0_0.1 was attributed to the formation of monosulfate (Ms) at the expense of ettringite, meanwhile, monocarbonate (Mc) and hemicarbonate (Hc) could be precipitated in LS10_0.1 and LS20_0.1 due to the presence of limestone [4,52,53]. The heat of pastes ground with DEIPA was emitted more than those without DEIPA at the same limestone substitution. In addition, more heat of LS10_0.1 and LS20_0.1 was generated than LS0_0.1, indicating limestone powder participated in the hydration reaction.

3.3.2. *Thermogravimetry analysis*

Fig. 7 illustrates the thermogravimetric and derivative thermogravimetry data of hydrated pastes. After 6 and 12 h, LS0_0 had a similar or larger amount of bound water with LS0_0.1, while DEIPA increased the weight loss of PLC, especially between 60 °C - 90 °C, which indicates more ettringite formation. On the first day of hydration, all pastes with DEIPA showed a lower degree of hydration at the same limestone substitution, moreover, gypsum was not fully dissolved in the pastes with GA. In the absence of limestone, DEIPA decreased weight loss within 300 °C, indicating less formation of C-S-H and ettringite on the first day.

The weight loss of AFm phases was observed after 3 days and onwards in the presence of DEIPA. Then, at the later ages of hydration, the weight loss when DEIPA was used was more pronounced, which suggests that more C-S-H, AFm phases, and siliceous hydrogarnet [40,54] had formed and points toward a higher degree of hydration in the long-term for the pastes ground in the presence of DEIPA. However, albeit the chemically bound water was higher in all pastes with DEIPA, less CH was observed independent of the presence of limestone.

3.3.3. *X-ray powder diffraction*

Fig. 8 shows the XRD patterns of hydrated pastes cured for 1, 3, 7, and 28 d, which is in agreement with the TG results (Fig. 7). The main hydration products common to all pastes were CH, C-S-H, and ettringite, and the clinker that remained in the later age was almost C_2S. After the first day of hydration, CH was not observed in the activated pastes. Moreover, the peak intensity of CH in the pastes without DEIPA to (0 0 1) direction was significantly higher than that in activated pastes during all hydration days (i.e., preferred orientation), which will be discussed later.

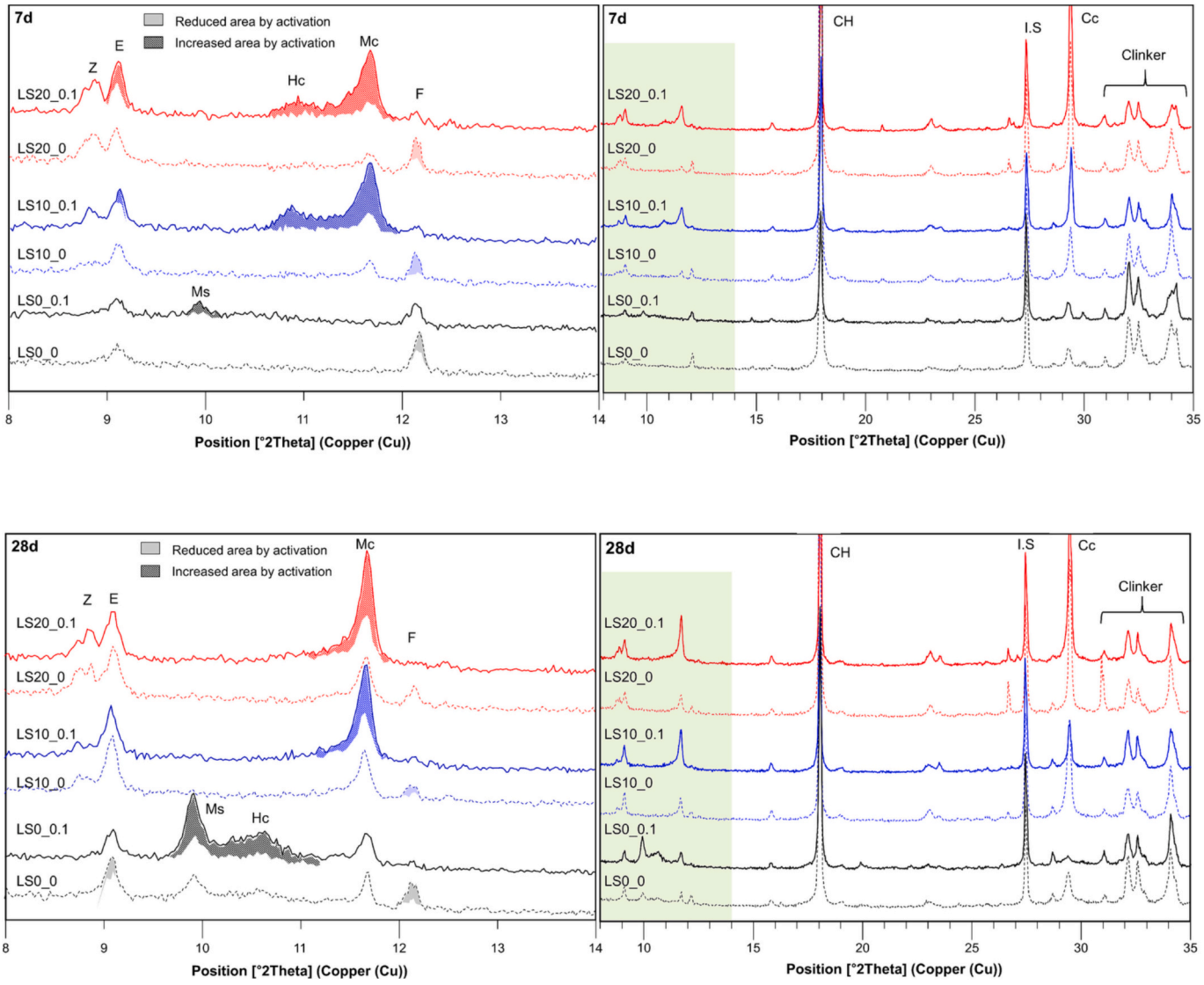

Fig. 8. (*continued*).

Since the presence of limestone and DEIPA has an effect on the AFm phase formation, XRD patterns between 8 and 14° 2θ degrees (CuKα) are also displayed in Fig. 8. The gypsum had only partially dissolved in the activated pastes after 1 day, indicating that DEIPA slowed down the dissolution of gypsum when it was employed as grinding agent. In addition, the gypsum in LS20_0 also remained because of the higher gypsum-to-clinker ratio. Despite the incomplete gypsum dissolution by the mechanochemical activation on 1 day, the peak intensity of ettringite hardly showed any difference between the pastes.

The peaks of AFm phases were observed after 3 days and onward in the activated pastes, but not in the pastes without DEIPA. In the absence of limestone, Ms. was slowly formed even in the activated pastes as the peak of Ms. was not detected until 7 days of hydration and it just showed a hump around 10° on 3 days. On the other hand, the Mc peak was clearly observed even after 3 days and Hc, in which the CO_3^{2-} in the interlayer is partially substituted with OH-, was also detected after 7 days in the activated PLC pastes. Thus, the mechanochemical activation, especially under the presence of limestone, enhanced C_4AF dissolution, leading to more formation of voluminous phases (i.e., AFm phases).

Finally, after 28 days of hydration, most of C_4AF was dissolved in the activated pastes while a portion of it remained in the unactivated pastes, resulting in a noticeable difference in the AFm formation between the pastes ground with and without DEIPA. The peak of Hc disappeared in activated PLC, which means calcite reacted further after 7 days of hydration. Meanwhile, the formation of Hc and Ms., which might be because of natural carbonation, was observed in LS0_0.1 [55].

In the absence of limestone powder, the enrichment of available alumina from C_4AF caused the decomposition of ettringite, one of the voluminous phases in cement paste. Whereas, the presence of limestone stabilized the ettringite as Mc is more stable than Ms., which indirectly gave rise to an increase of compressive strength in PLC pastes (Fig. 1) [4,52].

4. Discussion

4.1. Effect of grinding agent on mechanical activation

The Rietveld results of the all binder system were displayed in Fig. 9 and Table. 4. The amorphous contents increased in all binders after the grinding process, which is consistent with previous studies [56,57]. The presence of limestone powder under the activation affected the amorphization of the binder as well as particle size distribution and SSA.

In the absence of limestone, amorphous content increased and, especially, the silicate clinker contents were reduced more in LS0_0 (Fig. 4). Snellings et al., reported that the wet-grinding process with isopropanol decreased the amorphous content in cement while Kang

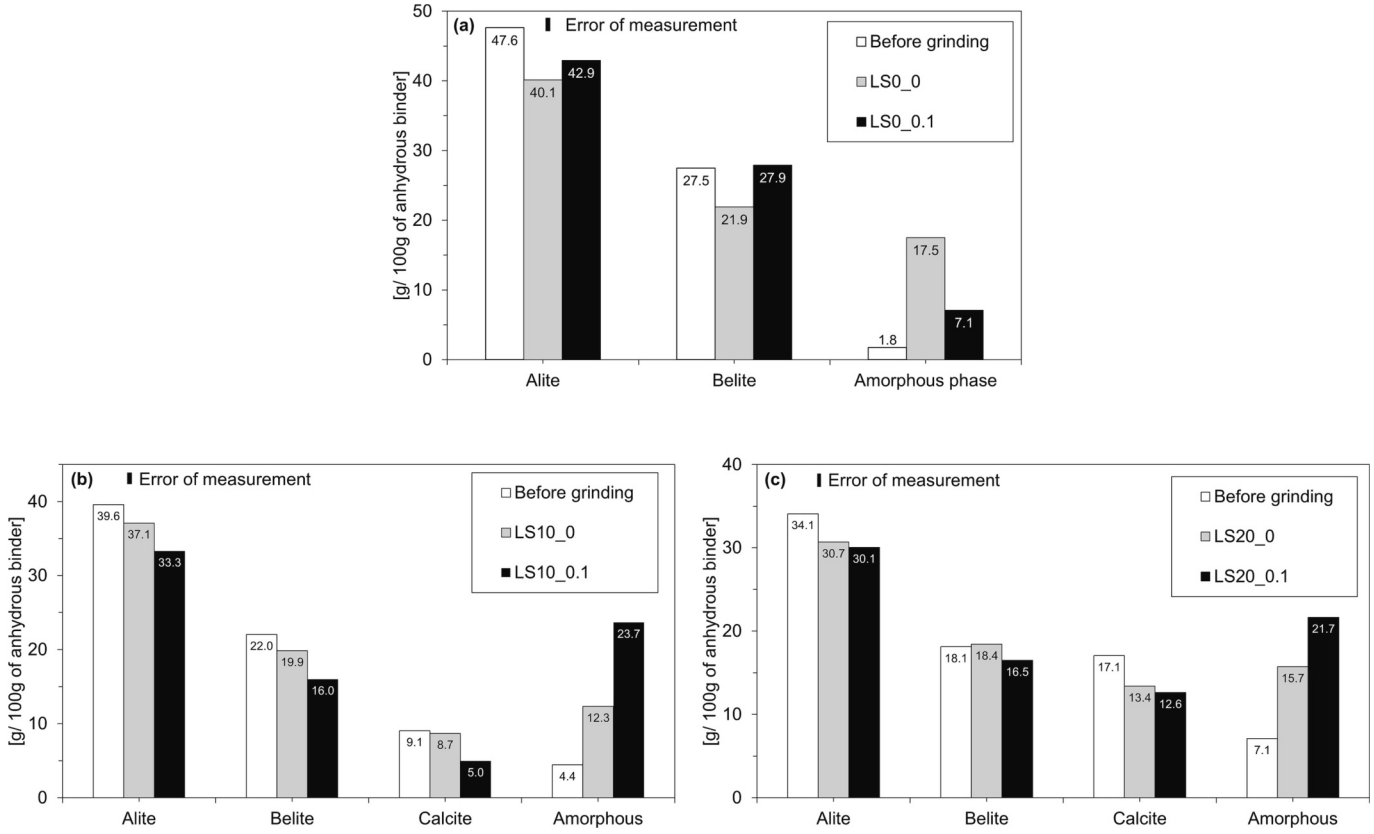

Fig. 9. Evolution of mineralogical phases before and after grinding process in PLC with (a) 0 %, (b) 10 % and (c) 20 % limestone substitution.

Table 4
Rietveld results before and after grinding with and without GA.

	0 % limestone substitution (wt%)			10 % limestone substitution (wt%)			20 % limestone substitution (wt%)		
	BG	LS0_0	LS0_0.1	BG	LS10_0	LS10_0.1	BG	LS20_0	LS20_0.1
C_3S	47.62	40.14	42.93	39.60	37.09	33.30	34.09	30.68	30.05
C_2S	27.50	21.90	27.91	22.04	19.86	18.53	18.11	18.42	16.48
C_3A	2.57	2.27	2.56	2.21	2.12	1.83	2.24	2.52	2.14
C_4AF	10.17	10.18	10.55	8.40	8.90	9.03	7.99	7.65	6.99
Calcite	–	–	–	9.05	8.69	4.97	17.05	14.39	12.62
Amorphous phase	1.75	17.51	7.10	4.44	12.34	23.67	7.10	15.72	21.65

et al. demonstrated that the dry-grinding transformed silicate clinker to the nano-crystalline phases, leading to the increase in amorphous contents [57,58]. In this study, the grinding process without GA could be considered as 'dry-grinding', thus, the amorphization of silicate phases was observed in LS0_0. Conversely, this effect was not pronounced in the presence of DEIPA because the liquid-type GA reduced friction during grinding.

Meanwhile, the mechanical effect on PLC was quite different with limestone-free cement. The amorphization or nano-crystallization of calcite can be achieved by mechanical process (i.e. milling), contributing to the increase of SSA and amorphous content in PLC [59,60]. In 10 % limestone substitution, furthermore, the reductions of C_3S and C_2S contents, as well as calcite, were also more prominent in the use of DEIPA. Sohoni et al. reported that 4.3 % of gypsum in clinker acts as a GA during its pulverization and the presence of gypsum enhances the grinding effect of alkanolamine GA [61]. In the same way, the limestone powder behaved as GA and this effect was improved with the presence of DEIPA. In 20 % limestone replacement, the results were similar to 10 % replacement, however, the amorphization of clinker was not as much, which might be because of insufficient grinding time with a relatively larger amount of limestone.

4.2. Effect of grinding agent on the early hydration of limestone-free cement

Fig. 10 illustrates the evolution of various mineralogical phases in the pastes without limestone with and without GA for up to 3 days. The retardation effect of DEIPA in the onset of hydration was most significant in the absence of limestone, and the retarded dissolution of C_3S continued until 3 days. This effect of DEIPA was observed in the previous studies, in which DEIPA was used as an additive (and not as a grinding agent) [15–17]. Ramanchandran et al. suggested that the adsorption of alkanolamines on hydrating C_3S produces a thick layer that interrupts the hydration of C_3S, blocking the contact between water and clinker [11]. Thus, the reduced dissolution of C_3S lowered the main hydration for 24 h.

Meanwhile, in the activated pastes, the C_4AF dissolution was also delayed until 1 day, however, it was accelerated later due to the complexation effect of DEIPA, resulting in a higher release of aluminum (note that C_4AF contained a high amount of aluminum) and the formation of AFm phase, which elucidates the shoulder of the activated paste. The improvement in the compressive strength after 3 days was also attributed to the formation of AFm phase, which was also caused by

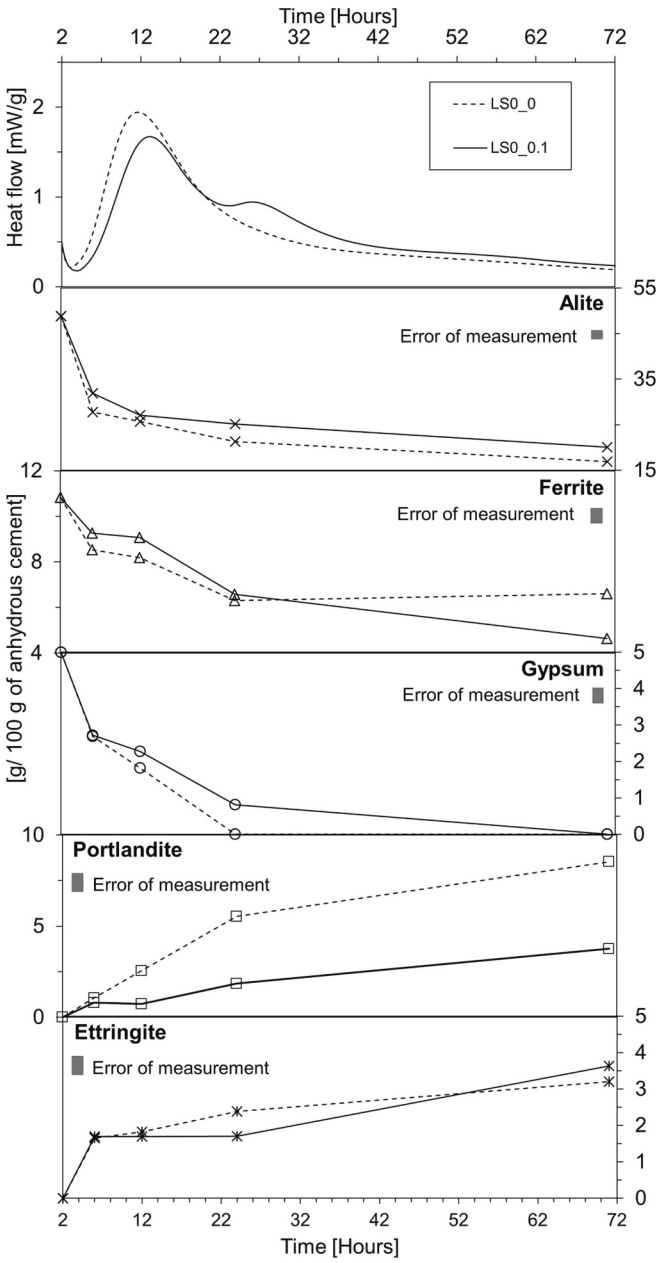

Fig. 10. Evolution of various mineralogical phases of limestone-free cement pastes with or without using grinding agent during early hydration.

C_4AF. In contrast, no clear shoulder or peak of secondary hydration was observed for the LS0_0. Note that the clinker used in the present study is rich in C_4AF but just contains 4 wt% of C_3A. Thus, the molar ratio of SO_3 (from gypsum) to Al_2O_3 (from C_3A and C_4AF), was high: SO_3/Al_2O_3 = 3.66 for LS0_0 after 3 days of hydration, determined based on XRF and Rietveld analysis [48,52], such that no significant amount of AFm was formed at a low degree of C_4AF reaction.

Lu et al. reported that a 0.1 % dosage of DEIPA accelerated the C_4AF dissolution and also retarded the silicate reaction during 3 days of hydration when DEIPA was used as an additive only [17]. In the present study where DEIPA was used as a GA, also delayed C_3S dissolution and the enhanced dissolution of C_4AF was observed, indicating that the impact of DEIPA on C_3S and C_4AF is similar regardless of the application type of DEIPA (i.e., additive vs. GA).

The effect on gypsum dissolution was quite different when DEIPA was used as GA. Many studies about DEIPA [15–17] reported that the addition of DEIPA accelerated the dissolution of gypsum. However, the use of DEIPA as GA delayed it, leading to a slightly lower ettringite formation on 1 day. After the gypsum dissolultion, almost the same amount of ettringite was formed in both. Albeit the secondary shoulder observed in the heat flow measurements (Fig. 6) and XRD patterns (Fig. 8) in the activated paste after 3 days, the amount of Ms. was small due to the slow formation at room temperature [62,63].

4.3. *Effect of grinding agent on the early hydration of Portland limestone cement*

Fig. 11 shows the evolution of various mineralogical phases in the PLC pastes with and without GA for up to 3 days. In the absence of DEIPA, the limestone replacement retarded the onset of hydration in the absence of GA due to a high gypsum-to-clinker ratio. Less clinker leads to higher effective water to clinker ratio, which retards the onset of the clinker reaction [64]. On the other hand, in the presence of DEIPA, the onset of hydration was accelerated as the limestone substitution increased. When PLC was ground with DEIPA, a portion of small particles, especially calcite and C_3S, increased (Table. 4 and Fig. 9). The improvement of surface area with the synergistic effect of limestone nucleation led to the accelerated hydration [64,65].

Fig. 11 (a) illustrates the effect of DEIPA in PLC that contains 10 % of limestone. In the same way as limestone-free pastes, the hydration shoulder was observed in only LS10_0.1. When DEIPA was used, the dissolution of C_3S was slightly delayed up to 6 h, but after 12 h, it was similar. In addition, C_4AF reaction enhanced more in LS10_0.1 than in LS0_0.1, indicating that limestone had a synergistic effect on the enhancement of C_4AF dissolution together with DEIPA. These effects led to a similar appearance time of hydration shoulder between LS0_0.1 and LS10_0.1, despite the higher quantity of gypsum per clinker. The presence of limestone and improved C_4AF reaction caused significant Mc formation in the activated PLC.

The impact of DEIPA as GA on the gypsum dissolution was the same for the sample with 10 % of limestone as for the cement without limestone. Initially, less gypsum had reacted and less ettringite was formed in LS10_0.1 than LS10_0 after 1 day, while more ettringite was observed for LS10_0.1 due to the larger gypsum to clinker ratio and the Mc formation after 3 days [4,52,53]. This formation of additional ettringite and AFm phase resulted in a higher compressive strength of LS10_0.1 after 3 days and onwards (Fig. 1).

Fig. 11(b) displays the effect of DEIPA in PLC with 20 % of limestone. The onset of LS20_0.1 hydration was almost the same as that of LS20_0, indicating that the acceleration effect of limestone with a larger SSA (Fig. 2) compensated for delaying effect of DEIPA. Moreover, the appearance of the shoulder, which was only well visible in the LS20_0.1, was also similar to the other activated pastes in spite of the highest relative amount of gypsum. During 3 days of hydration, the activated PLC emitted more heat, indicating the finer limestone produced by grinding with DEIPA actively participated in the hydration. The formation of hydration products (i.e., ettringite and Mc) also increased in LS20_0.1 due to the improved C_4AF, contributing to strength gain. Meanwhile, even in the 20 % limestone substitution, the retardation effect of DEIPA on gypsum dissolution was the same. In particular, the gypsum in LS20_0.1 hardly dissolved after 6 h compared to that in LS20_0. However, owing to the low clinker contents in LS20, the gypsum was not fully dissolved even after 1 day in both.

Despite the analogous C_3S dissolution after 3 days of hydration, less CH formation in all activated pastes was observed at the same amount of limestone; the CH in the unactivated pastes was twice as much as that of the activated pastes. The effect of alkanolamine additives on CH formation has been reported in many studies [15,16,66]. Zhang et al. proposed that distorted actinomorphic CH has a negative effect on early strength gain [9]. These outcomes are consistent with the TG and XRD results (Fig. 7 and Fig. 8) and support the comparably weak strength of activated pastes on 1 day (Fig. 1). The effect of grinding with DEIPA on the CH continued until the later age of hydration, which will be

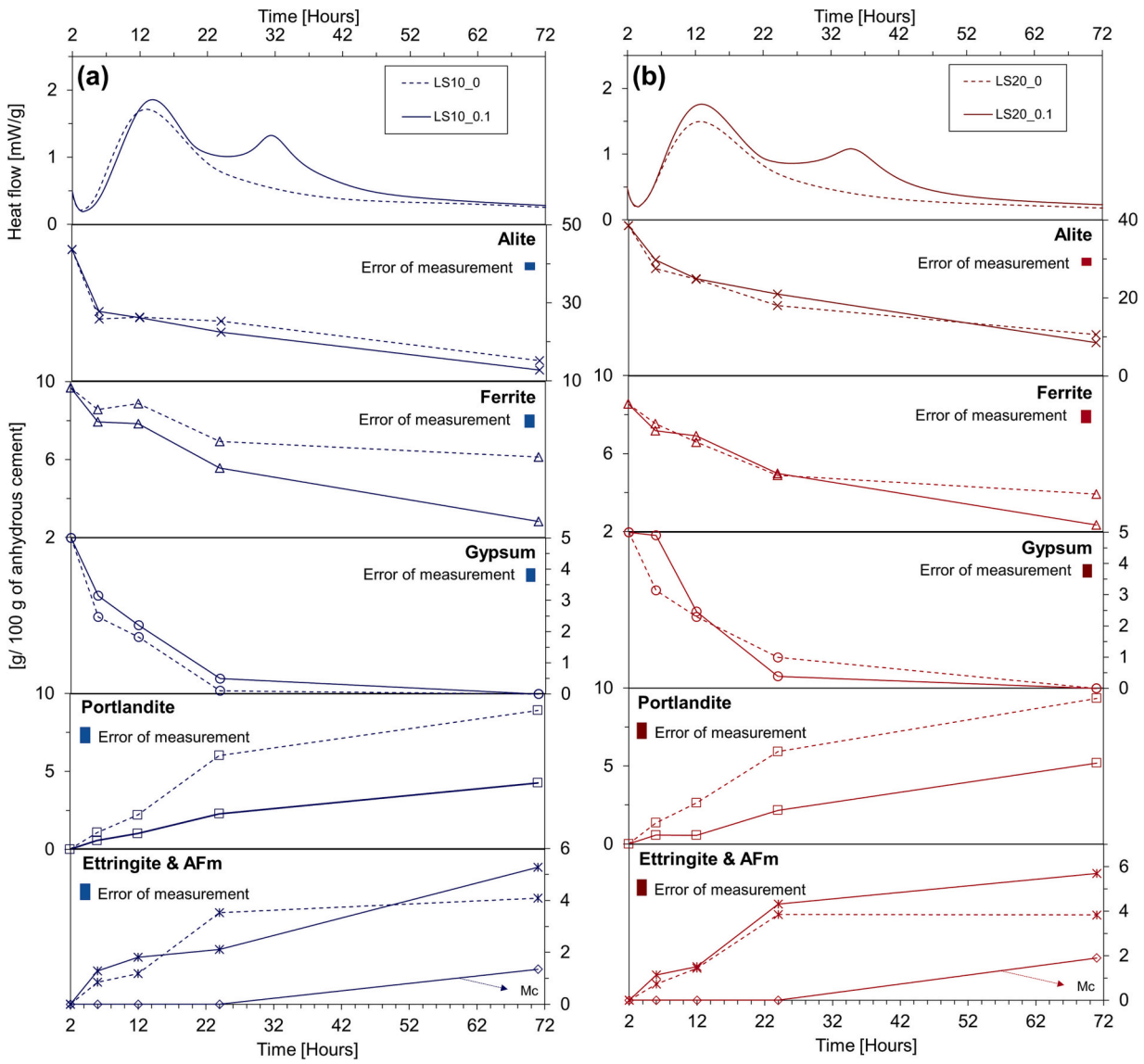

Fig. 11. Evolution of various mineralogical phases of Portland limestone cement pastes with or without using grinding agent during early hydration ((a): 10 % and (b): 20 % of limestone substitution).

discussed later in this paper.

4.4. *Effect of grinding agent on the later hydration*

Fig. 13 displays phase assemblages and weight losses of PLC after 28 d. In addition, the phase assemblages of other curing days (i.e., 1, 3, and 7 days) are included in the Supplementary Materials. C_3A in all pastes has reacted while a considerable portion of C_2S remained. All pastes that were ground with GA showed a larger weight loss between 20 and 400 °C than that of the pastes without GA on 28 d, which indicates the formation of more hydration products such as ettringite, AFm phases, and siliceous hydrogarnet. This high amount of bound water in the pastes with GA contributed to the higher compressive strength.

Since C_4AF in the clinker was alumina-rich, the improvement in C_4AF dissolution by the activation led to more formation of AFm phases, which caused the compressive strength enhancement. [53,67]. However, in the absence of limestone, DEIPA increased Ms. formation at the expense of ettringite. Since ettringite is the most voluminous, water rich material in the hydration products, the decomposition of ettringite has a negative effect on the strength. Thus, the mechanochemical activation on the limestone-free cement was not such pronounced for improving strength as much as on PLC.

In the presence of limestone, GA enhanced the C_4AF reaction and formation of Mc, indicating that the use of DEIPA as GA induced the noticeable participation of calcite in the hydration. In addition, more ettringite formed in the activated PLC, especially LS20_0.1, due to the stabilization effect of Mc and the higher relative gypsum content per clinker [4,52,67]. As more Mc formed, also slightly more calcite reacted, however, the amount of reacted calcite was limited consistent with previous studies [4–6]. A similar amount of Mc was formed in both LS10_0.1 and LS20_0.1 albeit the alumina content was the lowest in the LS20. It was because C_4AF was most dissolved in LS20_0.1 and the SSA of it was highest among all binders by mechanochemical activation. This increased Mc and ettringite formation in activated PLC was expected to contribute to the strength gain of PLC despite the 20 % of limestone substitution, since Mc can enhance the compressive strength by densifying the microstructure [5,6,68] and indirectly stabilizing the ettringite [4,52].

The TG after 28 days of hydration is represented in Fig. 13; the increased of weight loss between 200 and 400 °C was observed in the activated pastes. In the presence of DEIPA, the silicate reaction at the early age was somewhat delayed. In addition, more amorphous content,

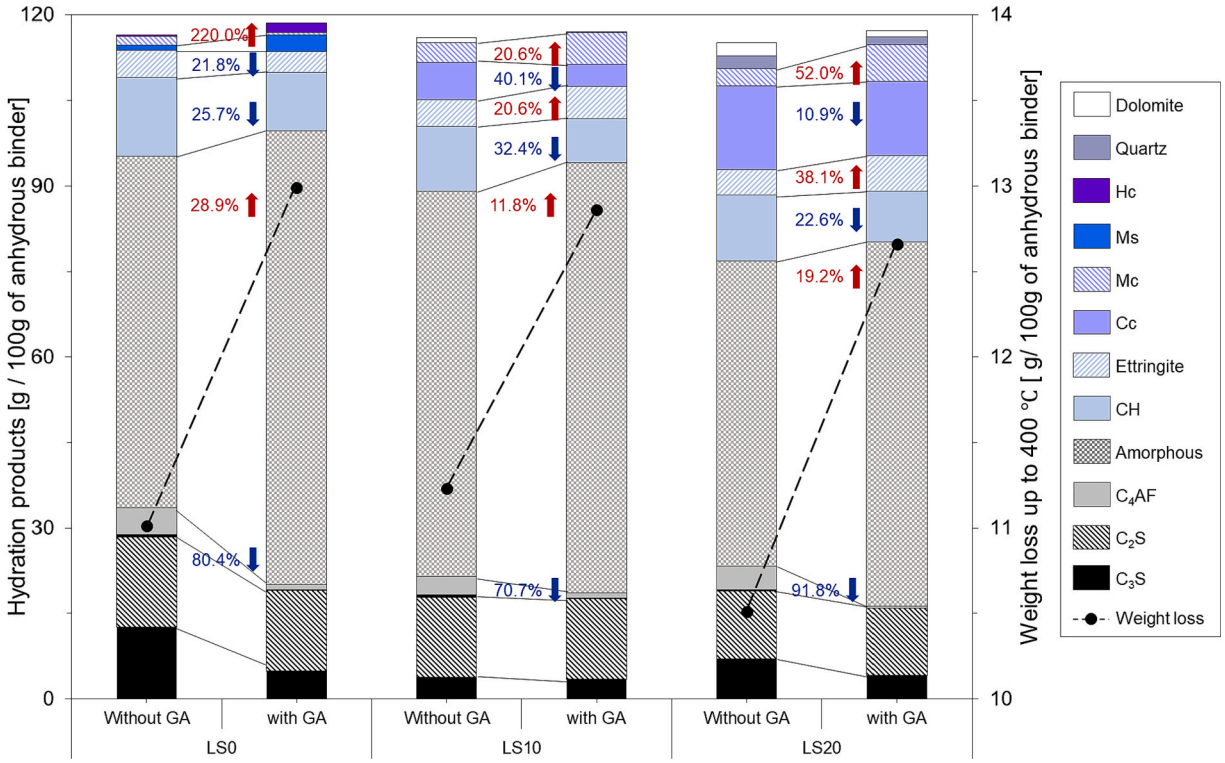

Fig. 12. Phase assemblages and weight loss between 20 °C - 400 °C of PLC after 28 days of hydration (Ms: monosulfate, Mc: monocarboaluminate, Hc: hemicarboaluminate).

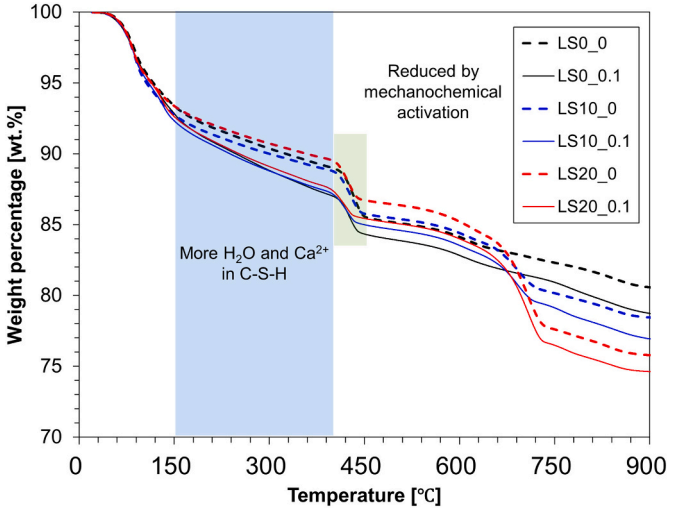

Fig. 13. TG data for hydrated cement after 28 days.

mainly C-S-H, but significantly less CH was observed after 28 days of hydration (Fig. 12). It seems that DEIPA allowed the uptake of more Ca^{2+} and water into C-S-H, preventing the precipitation of CH. In fact, Rinding et al. observed that the C/S ratio in C-S-H when DEIPA was used increased compared to the samples without DEIPA using EDX analysis [69]. The weight loss of C-S-H between 200 and 400 °C increases with C/S ratio [70], which would consistent with the higher weight loss of the pastes with DEIPA in this paper, and supports that the lower CH content is related to higher Ca^{2+} uptake in C-S-H.

4.5. *Effect of grinding agent on portlandite*

The CH formation during hydration was listed in Fig. 14, which was measured by TGA and Rietveld method; the results from Rietveld analysis and TGA were well-matched. Coupling with the result of TG and Rietveld analysis, The CH formation in the activated pastes during all hydration days was lower than that of the pastes without GA, indicating that DEIPA did not only inhibit the growth to (0 0 1) direction but also prevent its formation. For instance, the CH formation was lowered by about 30 % after 28 days of hydration, moreover, the variation of (0 0 1) peak intensity was almost twice in the XRD patterns, underlining the strong reduction of preferred orientation in the presence of DEIPA.

Fig. 15 (a) displays the effect of GA on the preferred orientation of CH and Fig. 15 (b) shows the reference pattern of CH. As shown in Fig. 8, The preferred orientation of CH to (0 0 1) direction in the unactivated pastes was observed during all hydration times, which causes a high anisotropy elastic modulus of CH in cement-based materials [71]. This preferred growth in (0 0 1) direction was substantially reduced in the presence of DEIPA as the alkanolamine-Ca^{2+} complexes the growth of CH [15,72]. Wang et al. observed irregular flake shaped CH, with lower crystallinity in the presence of alkanolamines, such as DEIPA and EDIPA [16].

4.6. *Siliceous hydrogarnet*

A selective extraction with SAM enables the better detection of Fe-containing phases by XRD as most other hydration products including CH are removed as illustrated in Fig. 16. (Al, Fe)-siliceous hydrogarnet ($Ca_3A_xF_{1-x}S_{0.84}H_{4.32}$) was observed, in agreement with other studies which identified it as the most stable Fe-containing hydration product in Portland cement [40,74,75]. As shown in Fig. 17, more (Al, Fe)-siliceous hydrogarnet was observed in LS0_0.1 due to the enhanced C_4AF dissolution than in LS0_0. Less (Al, Fe)-siliceous hydrogarnet was observed in the limestone containing pastes, even in LS20 pastes, the peaks of (Al, Fe)-siliceous hydrogarnet were hardly observed, which is partially

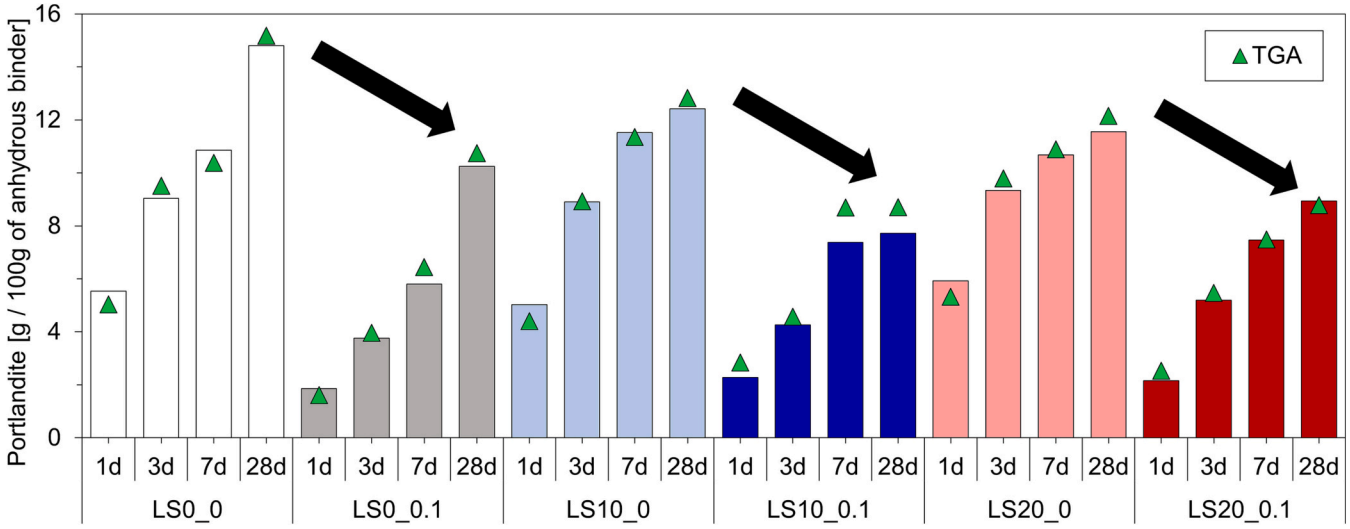

Fig. 14. Measured amount of portlandite in hydrated cement using Rietveld method and thermogravimetric analysis.

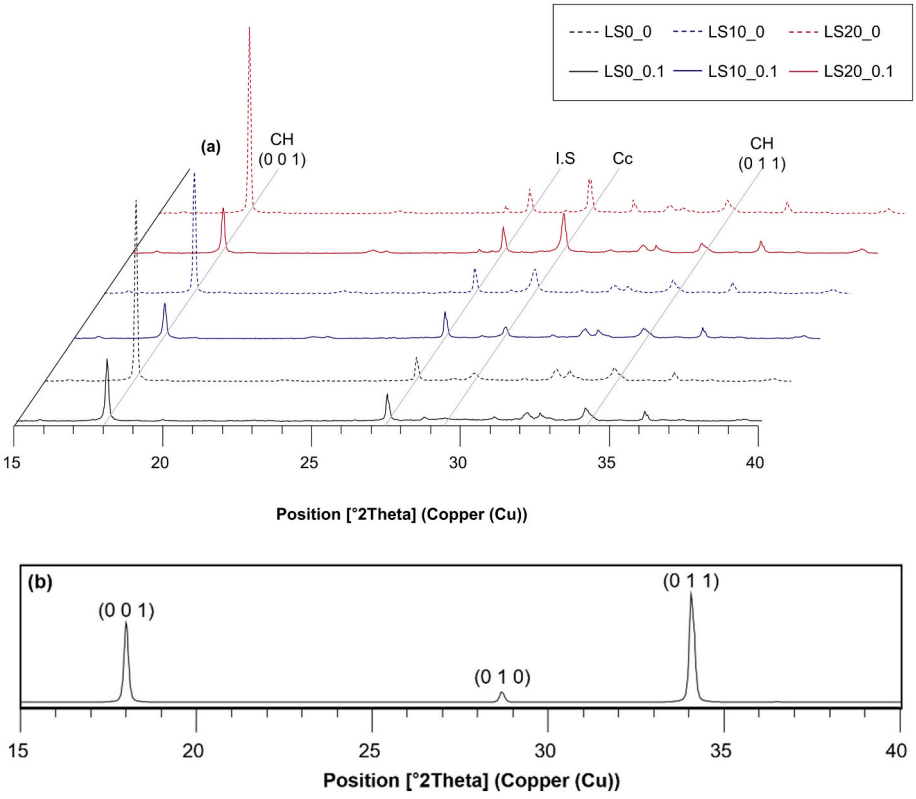

Fig. 15. XRD patterns (a) that containing the peak of portlandite after 28 days of hydration and (b) reference pattern of portlandite [PDF number of the COD reference patterns: 96–100-8782] [73] (CH: portlandite, I.S: internal standard material (TiO_2), $C\overline{C}$: calcite).

because of the lower amount of clinker.

The intensities of the peaks at 17.5° and 20.5° 2 θ associated with (Al, Fe)-siliceous hydrogarnet are similar, which indicates a comparable amount of Al and Fe in the siliceous hydrogarnet (Al siliceous hydrogarnet has a more intense band at 17.5°, while Fe-siliceous hydrogarnet has a more distinct band at 20.5° 2 theta) [40,74,75]. No significant effect of DEIPA on the Al and Fe ratio in siliceous hydrogarnet was observed, indicating that DEIPA just increased C_4AF reaction but had no impact on the Fe-containing hydration products. The 20 % surplus of Al present in C_4AF (Table 2), is expected to have contributed to additional Mc formation observed in the activated pastes.

4.7. Phase assemblages

Thermodynamic modeling was used to predict the hydrate assemblage based on the observed clinker reaction degree observed after 1 day and 28 days as illustrated in Fig. 17 and Fig. 18, respectively. The hydration degree of clinker and thermodynamic modeling of each curing day are presented in the Supplementary Materials. After 1 day of hydration, the volume of hydration product volume in the activated pastes was smaller, especially C-S-H and ettringite, than that of the unactivated pastes. Thus, the mechanochemical activation retarded the dissolution of clinker, leading to the bare formation of hydration products in the

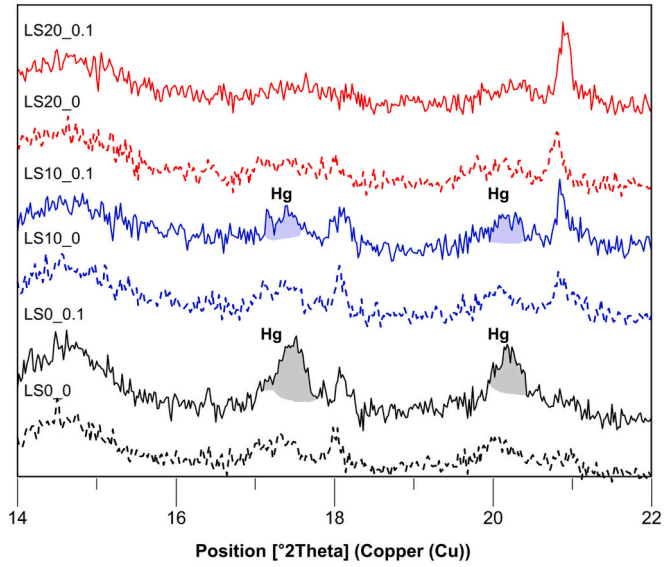

Fig. 16. XRD patterns after the selective dissolution method on 28 days of hydration (F: ferrite, Hg: (Al, Fe)-siliceous hydrogarnet).

activated pastes. The modeling also indicates, in line with the experimental results, that no AFm phases formed in all pastes after 1-day curing as C_3A dissolution did not fully progress.

After 28 days of hydration, the modeling suggests, in agreement with the experimental observation, that only a minor fraction of calcite reacted and that a small amount of AFm phases formed. It is also suggested that an increase in unreacted calcite lowered the total volume of hydrates, which contributed to the strength drop in PLC pastes without DEIPA. On the other hand, more formation of Mc was calculated in activated pastes than in the unactivated pastes due to the improved C_4AF dissolution. In addition, more C-S-H formation was calculated in the activated pastes, which might be because of the enhanced dissolution of C_3S by the DEIPA-Ca^{2+} complexation. It was also in agreement with the experimental results (i.e., higher amount of amorphous content). The results indicate that more (Al, Fe)-siliceous hydrogarnet was produced in the activated pastes, in line with the SAM result (Fig. 16). However, in both cases a similar amount of CH was calculated, as the increased Ca-content in C-S-H was not captured by the model due to a lack of thermodynamic data. The calculations showed a quite huge volume increase by mechanochemical activation, even though the increased Ca- and H_2O content in C-S-H and the hindrance effect of Ca^{2+}-DEIPA complex for the growth and production of CH could not simulated by the modeling [72].

5. Conclusion

In this paper, the mechanical change by using a grinding agent was confirmed through particle size distribution, the Blain surface area test, and X-ray diffraction analysis. Various experiments including Rietveld analysis, thermogravimetry analysis, hydration kinetics, and thermodynamic modeling were carried out to reveal the effect of using DEIPA as a grinding agent. Based on the findings of this study, the following conclusions can be obtained:

1. Mechanochemical activation by using 0.1 % DEIPA was significantly effective for grinding the Portland limestone cement than grinding just the clinker and gypsum. In the presence of limestone powder, the use of DEIPA increased the specific surface area and decreased the particle size as the limestone contents increased, while the effect of DEIPA on grinding limestone-free cement was not much noticeable.
2. Due to the higher grindability of limestone powder, limestone became smaller particles than clinker after grinding. In addition, the presence of limestone, under the use of DEIPA, led to the amorphization of silicate phases in clinker with itself after grinding. Conversely, when the limestone powder was not involved during grinding, the amorphous content increased rather in the absence of DEIPA.
3. In spite of mechanochemical activation, DEIPA retarded hydration and gypsum dissolution during the first day of hydration in all pastes. This effect on the dissolution of gypsum did not correspond with the previous studies, in which DEIPA was used as an additive. Meanwhile, the alite and ferrite dissolution at a later age was substantially improved when DEIPA was used. In the presence of limestone, the dissolution of ferrite was accelerated, resulting in the fast formation of more monocarbonate.
4. The compressive strength of all mechanochemically activated pastes was lowered after the first day owing to the delayed hydration. However, the strength of PLC with DEIPA was superior to that without DEIPA after 3 days and onwards despite limestone substitution; The strength was improved by >100 % (i.e., 17.2 to 45.1 MPa and 15.2 to 36.6 MPa for 10 % and 20 % limestone substitution, respectively). As discussed, the main reasons include (1) enhanced ferrite and alite dissolution and, (2) the precipitation of dense hydration products (as visible by the increased bound water content).

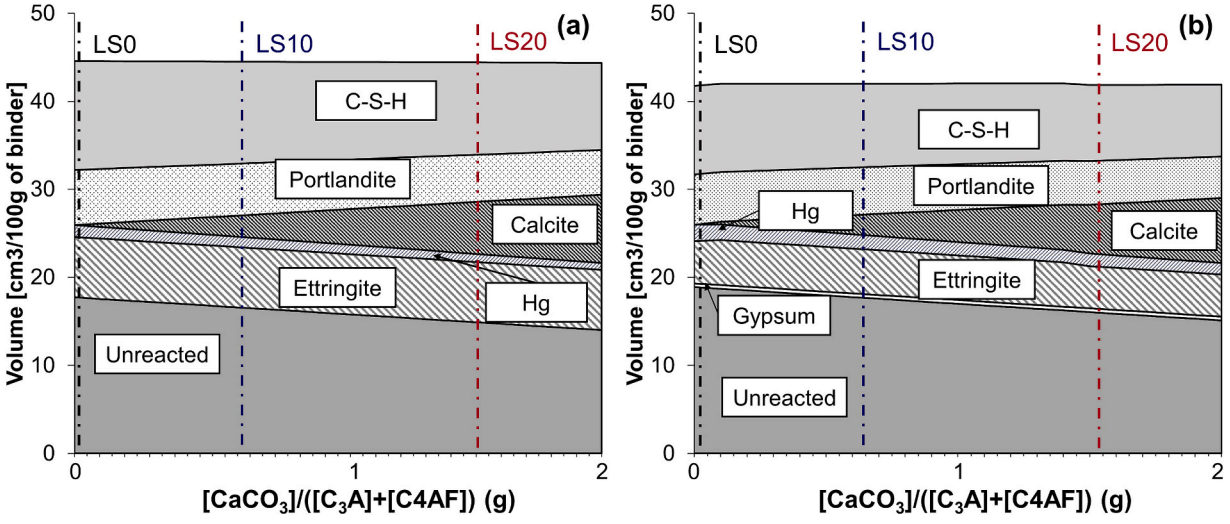

Fig. 17. Phase assemblages of (a) non-activated sample and (b) mechanochemically activated sample on 1 day (Hg: (Fe, Al)-siliceous hydrogarnet).

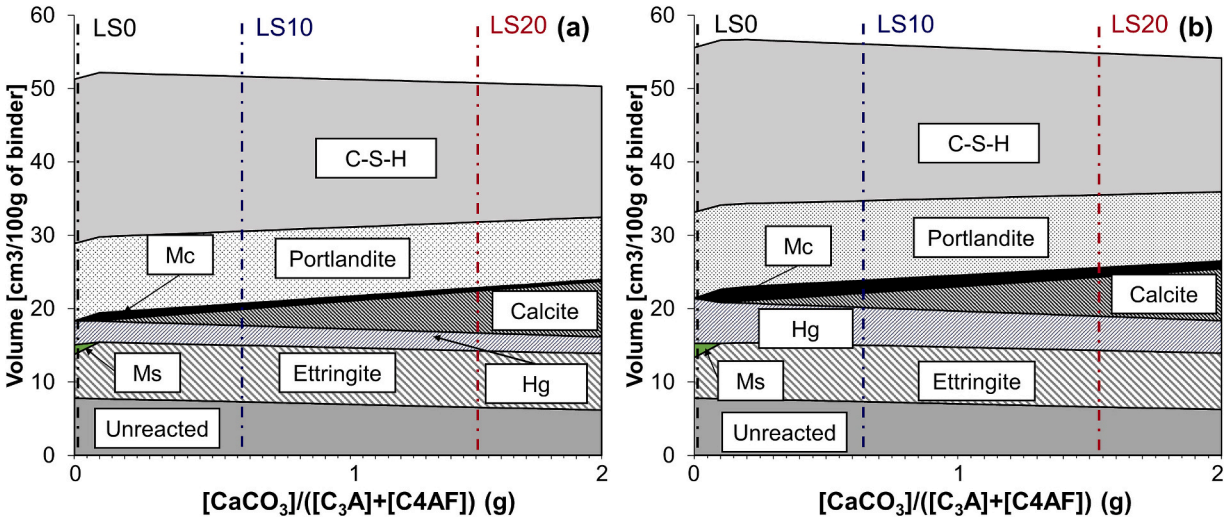

Fig. 18. Phase assemblages of (a) non-activated sample and (b) mechanochemically activated sample on 28 days (Hg: (Fe, Al)-siliceous hydrogarnet, Mc: monocarboaluminate, Ms.: monosulfate).

5. When the amount of gypsum was fixed at 5 wt%, the mechanochemical activation improved the compressive strength of PLC compared to the pastes without limestone, even with the 20 % limestone substitution. (1) The higher gypsum content and enhanced ferrite reaction promoted ettringite formation, (2) the enlarged specific surface area of limestone alleviated the formation of hydration products, and (3) monocarbonate stabilized the ettringite.
6. The mechanochemical activation had a clear impact on the calcium silicate reaction. The use of DEIPA as grinding agent did not only lead to the reduction of portlandite formation, but also decreased the preferred orientation to (0 0 1) direction during all curing days. However, it increased the C-S-H formation increased, especially on the later age of hydration, a higher Ca^{2+} and water uptake in C-S-H were observed in the activated pastes.
7. In summary, the investigation of mechanochemical activation should be conducted since, in the real cement manufacturing process, a grinding agent was applied during the pulverization process. In this study, the mechanochemical activation by using 0.1 % of DEIPA to Portland limestone cement can maintain the material performance even in 20 % of limestone substitution. The principles behind the reported improvement of Portland limestone cement are due to the enhanced specific surface area of limestone, the improved ferrite reactivity, the production of AFm phases, the stabilization of ettringite, and the generation of C-S-H with more Ca^{2+} and water, while less portlandite is formed.

CRediT authorship contribution statement

Jihoon Lee: Conceptualization, Data curation, Formal analysis, Investigation, Writing – original draft. **Barbara Lothenbach:** Validation, Writing – review & editing. **Juhyuk Moon:** Conceptualization, Funding acquisition, Validation, Writing – review & editing.

Declaration of competing interest

The authors declare that they have no known competing financial interests or personal relationships that could have appeared to influence the work reported in this paper.

Data availability

Data will be made available on request.

Acknowledgments

This work is supported by the Basic Science Research Program through the National Research Foundation of Korea (NRF) funded by the Ministry of Education, Republic of Korea (NRF-2021R1A2C4001944). The Institute of Engineering Research in Seoul National University provided research facilities for this work.

Appendix A. Supplementary data

Supplementary data to this article can be found online at https://doi.org/10.1016/j.cemconres.2023.107411.

References

[1] B. Lothenbach, K. Scrivener, R.D. Hooton, Supplementary cementitious materials, Cem. Concr. Res. 41 (12) (2011) 1244–1256.
[2] M.C.G. Juenger, R. Snellings, S.A. Bernal, Supplementary cementitious materials: new sources, characterization, and performance insights, Cem. Concr. Res. 122 (2019) 257–273.
[3] P. Hawkins, P.D. Tennis, R.J. Detwiler, The use of limestone in Portland cement: a state-of-the-art review, Portland Cement Association Skokie, IL, USA, 1996.
[4] B. Lothenbach, et al., Influence of limestone on the hydration of Portland cements, Cem. Concr. Res. 38 (6) (2008) 848–860.
[5] A.A. Ramezanianpour, et al., Influence of various amounts of limestone powder on performance of Portland limestone cement concretes, Cem. Concr. Compos. 31 (10) (2009) 715–720.
[6] A.M. Ramezanianpour, R.D. Hooton, A study on hydration, compressive strength, and porosity of Portland-limestone cement mixes containing SCMs, Cem. Concr. Compos. 51 (2014) 1–13.
[7] Z. Xu, et al., Research on cement hydration and hardening with different alkanolamines, Constr. Build. Mater. 141 (2017) 296–306.
[8] X.-M. Kong, et al., Influence of triethanolamine on the hydration and the strength development of cementitious systems, Mag. Concr. Res. 65 (18) (2013) 1101–1109.
[9] Y. Zhang, et al., Influences of triethanolamine on the performance of cement pastes used in slab track, Constr. Build. Mater. 238 (2020), 117670.
[10] Z. Lu, et al., Towards a further understanding of cement hydration in the presence of triethanolamine, Cem. Concr. Res. 132 (2020), 106041.
[11] V.S. Ramachandran, Influence of triethanolamine on the hydration characteristics of tricalcium silicate, J. Appl. Chem. Biotechnol. 22 (11) (1972) 1125–1138.
[12] P.J. Sandberg, F. Doncaster, On the mechanism of strength enhancement of cement paste and mortar with triisopropanolamine, Cem. Concr. Res. 34 (6) (2004) 973–976.
[13] H. Huang, X.-D. Shen, Interaction effect of triisopropanolamine and glucose on the hydration of Portland cement, Constr. Build. Mater. 65 (2014) 360–366.
[14] B. Ma, et al., Effect of triisopropanolamine on compressive strength and hydration of cement-fly ash paste, Constr. Build. Mater. 179 (2018) 89–99.
[15] S. Ma, et al., Study on the hydration and microstructure of Portland cement containing diethanol-isopropanolamine, Cem. Concr. Res. 67 (2015) 122–130.
[16] Y. Wang, et al., Effect of diethanolisopropanolamine and ethyldiisopropylamine on hydration and strength development of Portland cement, Cem. Concr. Res. 162 (2022).

[17] Z. Lu, et al., A comparative study of the effects of two alkanolamines on cement hydration, Adv. Cem. Res. 34 (2) (2022) 47–56.
[18] M. Ali, R. Saidur, M. Hossain, A review on emission analysis in cement industries, Renew. Sust. Energ. Rev. 15 (5) (2011) 2252–2261.
[19] S. Fellaou, T. Bounahmidi, Evaluation of energy efficiency opportunities of a typical Moroccan cement plant: part I, Energy analysis. Appl. Therm. Eng. 115 (2017) 1161–1172.
[20] S. Fellaou, T. Bounahmidi, Analyzing thermodynamic improvement potential of a selected cement manufacturing process: advanced exergy analysis, Energy 154 (2018) 190–200.
[21] W. Li, et al., The mechanochemical process and properties of Portland cement with the addition of new alkanolamines, Powder Technol. 286 (2015) 750–756.
[22] L. Opoczky, Grinding technical questions of producing composite cement, Int. J. Miner. Process. 44 (1996) 395–404.
[23] M. Katsioti, et al., Characterization of various cement grinding aids and their impact on grindability and cement performance, Constr. Build. Mater. 23 (5) (2009) 1954–1959.
[24] A. Marzouki, et al., The effects of grinding on the properties of Portland-limestone cement, Constr. Build. Mater. 48 (2013) 1145–1155.
[25] H.M. Rietveld, A profile refinement method for nuclear and magnetic structures, J. Appl. Crystallogr. 2 (2) (1969) 65–71.
[26] L. Girotto, et al., Extraction of tricalcium aluminate for research applications by selective dissolution of Portland cement clinker, J. Mater. Civ. Eng. 32 (1) (2020) 04019325.
[27] H. Kang, et al., Mechanochemical effect of alkanolamines on the C4AF: crystal structure, hydration behavior, and strength enhancement, Cem. Concr. Compos. 145 (2024), 105326.
[28] H. Kim, et al., Neutron and X-ray diffraction study of pyrophosphate-based Li2–x MP2O7 (M= Fe, Co) for lithium rechargeable battery electrodes, Chem. Mater. 23 (17) (2011) 3930–3937.
[29] L. Finger, D. Cox, A. Jephcoat, A correction for powder diffraction peak asymmetry due to axial divergence, J. Appl. Crystallogr. 27 (6) (1994) 892–900.
[30] A. Gualtieri, et al., Rietveld refinement using synchrotron X-ray powder diffraction data collected in transmission geometry using an imaging-plate detector: application to standard m-ZrO2, J. Appl. Crystallogr. 29 (6) (1996) 707–713.
[31] B. Marler, A. Grünewald-Lüke, H. Gies, Structure refinement of the as-synthesized and the calcined form of zeolite RUB-3 (RTE), Microporous Mesoporous Mater. 26 (1–3) (1998) 49–59.
[32] J. Zhang, G.W. Scherer, Comparison of methods for arresting hydration of cement, Cem. Concr. Res. 41 (10) (2011) 1024–1036.
[33] H. Kang, J. Moon, Secondary curing effect on the hydration of ultra-high performance concrete, Constr. Build. Mater. 298 (2021).
[34] R. Snellings, et al., Report of TC 238-SCM: hydration stoppage methods for phase assemblage studies of blended cements—results of a round robin test, Mater. Struct. 51 (4) (2018) 1–12.
[35] K. Scrivener, R. Snellings, B. Lothenbach, A Practical Guide to Microstructural Analysis of Cementitious Materials Vol. 540, Crc Press Boca Raton, FL, USA, 2016.
[36] K. De Weerdt, et al., Hydration mechanisms of ternary Portland cements containing limestone powder and fly ash, Cem. Concr. Res. 41 (3) (2011) 279–291.
[37] R. Allmann, R. Hinek, The introduction of structure types into the inorganic crystal structure database ICSD, Acta Crystallogr. A: Found. Crystallogr. 63 (5) (2007) 412–417.
[38] S. Gražulis, et al., Crystallography open database (COD): an open-access collection of crystal structures and platform for world-wide collaboration, Nucleic Acids Res. 40 (D1) (2012) D420–D427.
[39] D.L. Bish, S. Howard, Quantitative phase analysis using the Rietveld method, J. Appl. Crystallogr. 21 (2) (1988) 86–91.
[40] B.Z. Dilnesa, et al., Fe-containing phases in hydrated cements, Cem. Concr. Res. 58 (2014) 45–55.
[41] G. Le Saout, et al., Chemical structure of cement aged at normal and elevated temperatures and pressures: part I, Class G oilwell cement. Cement Concr. Res. 36 (1) (2006) 71–78.
[42] T. Wagner, et al., GEM-Selektor geochemical modeling package: TSolMod library and data interface for multicomponent phase models, Can. Mineral. 50 (5) (2012) 1173–1195.
[43] D.A. Kulik, et al., GEM-Selektor geochemical modeling package: revised algorithm and GEMS3K numerical kernel for coupled simulation codes, Comput. Geosci. 17 (1) (2013) 1–24.
[44] T. Thoenen, et al., The PSI/Nagra Chemical Thermodynamic Database 12/07, 2014.
[45] B. Lothenbach, et al., Cemdata18: a chemical thermodynamic database for hydrated Portland cements and alkali-activated materials, Cem. Concr. Res. 115 (2019) 472–506.
[46] D.A. Kulik, Improving the structural consistency of CSH solid solution thermodynamic models, Cem. Concr. Res. 41 (5) (2011) 477–495.
[47] H. Helgeson, Theoretical Prediction of the Thermodynamic Behavior of Aqueous Electrolytes by High Pressures and Temperatures; Iv, Calculation of Activity Coefficients, Osmotic Coefficients, and Apparent MOLAL and Standard and Relative Partial MOLAL Properties to 600OC and 5KB, 1981.
[48] B. Lothenbach, et al., Thermodynamic modelling of the effect of temperature on the hydration and porosity of Portland cement, Cem. Concr. Res. 38 (1) (2008) 1–18.
[49] T. Hirsch, Z. Lu, D. Stephan, Impact of triethanolamine on the sulfate balance of Portland cements with mixed sulfate carriers, J. Am. Ceram. Soc. 104 (9) (2021) 4829–4842.
[50] K. Vance, et al., Hydration and strength development in ternary Portland cement blends containing limestone and fly ash or metakaolin, Cem. Concr. Compos. 39 (2013) 93–103.
[51] Y. Briki, et al., Impact of limestone fineness on cement hydration at early age, Cem. Concr. Res. 147 (2021), 106515.
[52] T. Matschei, B. Lothenbach, F.P. Glasser, The role of calcium carbonate in cement hydration, Cem. Concr. Res. 37 (4) (2007) 551–558.
[53] A. Quennoz, K.L. Scrivener, Hydration of C3A–gypsum systems, Cem. Concr. Res. 42 (7) (2012) 1032–1041.
[54] H.F. Taylor, Cement Chemistry vol. 2, Thomas Telford London, 1997.
[55] F. Georget, et al., Stability of hemicarbonate under cement paste-like conditions, Cem. Concr. Res. 153 (2022), 106692.
[56] R. Mejdoub, et al., The effect of prolonged mechanical activation duration on the reactivity of Portland cement: effect of particle size and crystallinity changes, Constr. Build. Mater. 152 (2017) 1041–1050.
[57] H. Kang, et al., Importance of amorphous content, surface energy, and preferred orientation on the accurate quantification of cement minerals in clinkers, J. Build. Eng. 66 (2023), 105887.
[58] R. Snellings, A. Bazzoni, K. Scrivener, The existence of amorphous phase in Portland cements: physical factors affecting Rietveld quantitative phase analysis, Cem. Concr. Res. 59 (2014) 139–146.
[59] S. Leukel, et al., Mechanochemical access to defect-stabilized amorphous calcium carbonate, Chem. Mater. 30 (17) (2018) 6040–6052.
[60] T. Li, et al., Effects of dry grinding on the structure and granularity of calcite and its polymorphic transformation into aragonite, Powder Technol. 254 (2014) 338–343.
[61] S. Sohoni, R. Sridhar, G. Mandal, The effect of grinding aids on the fine grinding of limestone, quartz and Portland cement clinker, Powder Technol. 67 (3) (1991) 277–286.
[62] T. Matschei, B. Lothenbach, F. Glasser, The AFm phase in Portland cement, Cem. Concr. Res. 37 (2) (2007) 118–130.
[63] D. Damidot, F. Glasser, Thermodynamic investigation of the CaO·Al2O3·CaSO4·H2O system at 50° C and 85° C, Cem. Concr. Res. 22 (6) (1992) 1179–1191.
[64] A. Schöler, et al., Early hydration of SCM-blended Portland cements: a pore solution and isothermal calorimetry study, Cem. Concr. Res. 93 (2017) 71–82.
[65] J. Péra, S. Husson, B. Guilhot, Influence of finely ground limestone on cement hydration, Cem. Concr. Compos. 21 (2) (1999) 99–105.
[66] Y. Zhang, et al., A further understanding on the strength development of cement pastes in the presence of triisopropanolamine used in CRTS III slab track, Constr. Build. Mater. 315 (2022), 125743.
[67] T. Matschei, B. Lothenbach, F.P. Glasser, The AFm phase in Portland cement, Cem. Concr. Res. 37 (2) (2007) 118–130.
[68] C.W. Hargis, A. Telesca, P.J. Monteiro, Calcium sulfoaluminate (Ye'elimite) hydration in the presence of gypsum, calcite, and vaterite, Cem. Concr. Res. 65 (2014) 15–20.
[69] K. Riding, D.A. Silva, K. Scrivener, Early age strength enhancement of blended cement systems by CaCl2 and diethanol-isopropanolamine, Cem. Concr. Res. 40 (6) (2010) 935–946.
[70] R. Maddalena, et al., Direct synthesis of a solid calcium-silicate-hydrate (CSH), Constr. Build. Mater. 223 (2019) 554–565.
[71] Q. Zheng, et al., New insights into the role of portlandite in the cement system: elastic anisotropy, thermal stability, and structural compatibility with CSH, Cryst. Growth Des. 20 (4) (2020) 2477–2488.
[72] J. Wang, et al., Effect of chelating solubilization via different alkanolamines on the dissolution properties of steel slag, J. Clean. Prod. 365 (2022), 132824.
[73] W.R. Busing, H.A. Levy, Neutron diffraction study of calcium hydroxide, J. Chem. Phys. 26 (3) (1957) 563–568.
[74] B.Z. Dilnesa, et al., Iron in carbonate containing AFm phases, Cem. Concr. Res. 41 (3) (2011) 311–323.
[75] B.Z. Dilnesa, et al., Synthesis and characterization of hydrogarnet Ca3(AlxFe1−x)2 (SiO4)y(OH)4(3−y), Cem. Concr. Res. 59 (2014) 96–111.